

Inference for overparametrized hierarchical Archimedean copulas

Samuel Perreault^{†*} Yanbo Tang[‡] Ruyi Pan[†] Nancy Reid[†]

[†]University of Toronto, Canada [‡]Imperial College London, United Kingdom

November 15, 2024

Abstract

Hierarchical Archimedean copulas (HACs) are multivariate uniform distributions constructed by nesting Archimedean copulas into one another, and provide a flexible approach to modeling non-exchangeable data. However, this flexibility in the model structure may lead to over-fitting when the model estimation procedure is not performed properly. In this paper, we examine the problem of structure estimation and more generally on the selection of a parsimonious model from the hypothesis testing perspective. Formal tests for structural hypotheses concerning HACs have been lacking so far, most likely due to the restrictions on their associated parameter space which hinders the use of standard inference methodology. Building on previously developed asymptotic methods for these non-standard parameter spaces, we provide an asymptotic stochastic representation for the maximum likelihood estimators of (potentially) overparametrized HACs, which we then use to formulate a likelihood ratio test for certain common structural hypotheses. Additionally, we also derive analytical expressions for the first- and second-order partial derivatives of two-level HACs based on Clayton and Gumbel generators, as well as general numerical approximation schemes for the Fisher information matrix.

1 Introduction

Multivariate hierarchical modeling is an appealing and effective framework for capturing complex dependency structures in data. In particular, copula-based approaches have become increasingly popular, and many interesting and flexible copulas have been introduced reflect for a wide array of dependence structures. We focus on a sub-class of multivariate hierarchical models proposed in Joe (1997) called hierarchical Archimedean copulas (HACs), which are widely used in finance, insurance and risk management (Savu and Trede, 2010; Hofert and Scherer, 2011; Abdallah et al., 2015; Cossette et al., 2019b; Li et al., 2021). Our main purpose is to provide insights into the asymptotic behaviour of the maximum likelihood estimator (MLE) and likelihood ratio statistic within the framework of overparametrized HACs. We call a HAC overparametrized if it contains more parameters than needed to specify the true distribution.

*Corresponding author: samuel.perreault@utoronto.ca

As with many hierarchical models, a key barrier to the practical usage of HACs is in finding an appropriate tree structure (hierarchy) for the data at hand, one that is complex enough to capture the complexity of the data, but simple enough to prevent over-fitting. We provide a method for testing some important structural hypotheses for possibly overparametrized HACs through likelihood ratio statistic. In order to characterize the asymptotic distribution of the likelihood ratio, we need to consider parameters on the boundary of the parameter space, a setting which does not allow the use of standard inference methodology.

Our main result, Theorem 1, provides an asymptotic stochastic representation for the likelihood ratio statistic in these non-standard conditions, and thus partially extends Theorem 1 of Hofert et al. (2012) for Archimedean copulas, and Theorem 1.b of Okhrin et al. (2013), which deals with non-overparametrized HACs with parameters in the interior of the parameter space, and a multi-stage maximum likelihood estimation procedure.

1.1 Hierarchical Archimedean Copulas

As the name suggests, HACs are multivariate distributions with uniform margins whose building blocks are Archimedean copulas. A p -variate Archimedean copula C_θ with parameter θ is fully characterized by its generator ψ_θ via

$$C_\theta(\mathbf{u}) = \psi_\theta\{\phi_\theta(u_1) + \dots + \phi_\theta(u_p)\}, \quad \text{for all } \mathbf{u} \in [0, 1]^p, \quad (1)$$

where $\phi_\theta(s) := \inf\{t \in [0, \infty] : \psi_\theta(t) = s\}$ is the generalized inverse of ψ_θ . It was shown by McNeil and Nešlehová (2009) that an Archimedean copula C_θ is proper, in that it is a multivariate distribution with $U(0, 1)$ univariate margins, if and only if ψ_θ is d -monotone: a continuous function on $[0, \infty]$ admitting derivatives $\psi^{(k)}$ up to the order $k = d - 2$ satisfying $(-1)^k \psi^{(k)}(t) \geq 0$ for all $k \in \{0, \dots, d - 2\}$ and $t \in (0, \infty)$, and $(-1)^{d-2} \psi^{(d-2)}$ is decreasing and convex on $(0, \infty)$. Prime examples of d -monotone generators are the Clayton and Gumbel generators, respectively given by

$$\psi_\theta(t) = (1 + t)^{-1/\theta} \quad \text{and} \quad \psi_\theta(t) = \exp(-t^{1/\theta}), \quad (2)$$

where $\theta \in (0, \infty)$ for the Clayton generator and $\theta \in [1, \infty)$ for the Gumbel generator. These are in fact examples of completely monotone generators: infinitely differentiable generators whose derivatives satisfy $(-1)^k \psi^{(k)}(t) \geq 0$ for all $k \in \{0, 1, \dots\}$ and $t \in (0, \infty)$.

A HAC is constructed by nesting Archimedean copulas into one another, and is partially characterized by a tree whose leaf nodes each represent a unique variable. As illustrated in Figure 1, we index the nodes of this tree using vectors \mathbf{i} , which encodes the path to the corresponding node from the root, whose index is always (0) . We denote the set of all indices corresponding to non-leaf nodes by \mathcal{I} ; for all $\mathbf{i} \in \mathcal{I}$, $K_{\mathbf{i}}$ denotes the number of children of node \mathbf{i} (the nodes directly below \mathbf{i}) and $d_{\mathbf{i}}$ denotes the number of leaf nodes below it (the nodes below \mathbf{i} which has no child nodes). Using this notation, a HAC C can be represented recursively as

$$C^{\mathbf{i}}(\mathbf{u}) = C_{\mathbf{i}}\{C^{(\mathbf{i},1)}(\mathbf{u}_1), \dots, C^{(\mathbf{i},K_{\mathbf{i}})}(\mathbf{u}_{K_{\mathbf{i}}})\}, \quad \text{for all } \mathbf{i} \in \mathcal{I} \text{ and } \mathbf{u} = (\mathbf{u}_k \in [0, 1]^{d_{(\mathbf{i},k)}} : k = 1, \dots, K_{\mathbf{i}}), \quad (3)$$

where $C_{\mathbf{i}}$ is an Archimedean copula and $C^{(\mathbf{i},k)}$, $k = 1, \dots, K_{\mathbf{i}}$, are themselves HACs of lower-

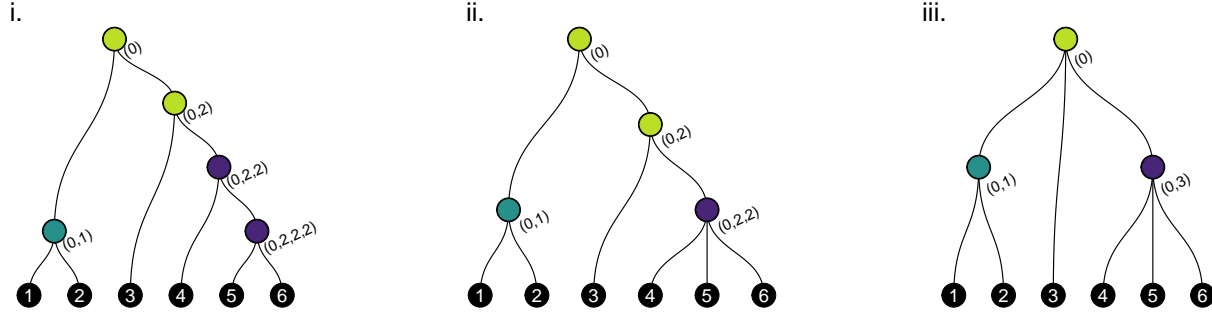


Figure 1: Some tree structures partially characterizing HACs. The indexing of the nodes is as described around (3). Each node corresponds to an Archimedean copula, which we assume is described by one parameter. When the Archimedean copulas associated to a parent-child pair of nodes are of the same type and have equal parameters, the child node can be collapsed into its parent. The tree in panel ii. is obtained by collapsing node $(0, 2, 2, 2)$ in panel i. and similarly, the tree in panel iii. is obtained by collapsing node $(0, 2)$ in panel ii.

fig:trees

dimensions; $C^{(0)} = C$ and $C^{(\mathbf{i},k)}$ is the identity function when (\mathbf{i}, k) is a leaf node. For each $\mathbf{i} \in \mathcal{I}$, we define $\psi_{\mathbf{i}}$ and $\phi_{\mathbf{i}}$ as the generator and inverse generator of $C_{\mathbf{i}}$ respectively, and $\theta_{\mathbf{i}}$ as the corresponding scalar parameter; $\boldsymbol{\theta} := (\theta_{\mathbf{i}})_{\mathbf{i} \in \mathcal{I}}$ is the full parameter vector.

In contrast with Archimedean copulas, non-trivial HACs are not exchangeable, which makes them much more attractive in real data settings, where exchangeability is often an unreasonable assumption. This increased flexibility, comes at the cost of additional theoretical considerations however; using Archimedean copulas as building blocks for a HAC does not necessarily yield a proper copula. To guarantee that a given HAC $C = C_{\boldsymbol{\theta}}$ is proper, one may verify the sufficient, but not necessary condition that, for any $\mathbf{i}, (\mathbf{i}, k) \in \mathcal{I}$, the parent-child composition $\phi_{\mathbf{i}} \circ \psi_{(\mathbf{i},k)}$ defines a completely monotone generator. For some families of completely monotone generators such as the Gumbel or Clayton, it suffices to check whether $\theta_{\mathbf{i}} \leq \theta_{(\mathbf{i},k)}$ (Holeňa et al. (2015), see also Table 2.3 in Hofert (2010)). This suggests restricting the parameter space $\Theta \subset \mathbb{R}^{|\mathcal{I}|}$ to

$$\Theta = \left\{ \boldsymbol{\theta} = (\theta_{\mathbf{i}})_{\mathbf{i} \in \mathcal{I}} \in \mathbb{R}^{|\mathcal{I}|} : \theta_{\mathbf{i}} \leq \theta_{(\mathbf{i},k)} \text{ for all } \mathbf{i}, (\mathbf{i}, k) \in \mathcal{I}, \text{ and } k \in \{1, \dots, K_{\mathbf{i}}\} \right\}, \quad (4)$$

eq:Theta

where Θ encodes further requirements on individual parameters imposed by specific generator families; for example, $\Theta = (0, \infty)$ and $\Theta = [1, \infty)$ for the Clayton and Gumbel families, respectively. See Figure 2.i for a depiction of Θ for two-parameter HACs. Although advances have been made on the topic, verifying that a HAC mixing many types of generators is a proper copula is difficult in general; see Rezapour (2015) and Holeňa et al. (2015) for sufficient conditions for constructing proper HACs through nesting, and Hering et al. (2010), Zhu et al. (2016) and Cossette et al. (2017) for construction methods that necessarily yields proper copulas.

The main issue we focus on arises when two or more parameters corresponding to neighbouring nodes, say \mathbf{i} and $(\mathbf{i}, 1)$, are equal, meaning that the parameter vector lies on the boundary of Θ . These cases are of particular interest, as $\phi_{\mathbf{i}} \circ \psi_{(\mathbf{i},k)}$ implicitly appearing in (3) then reduces to the

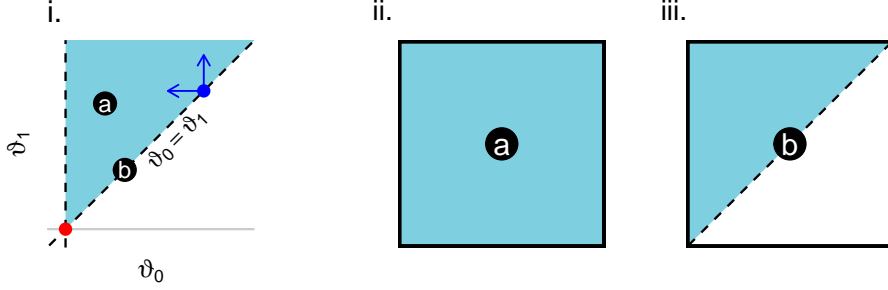


Figure 2: (i) Depiction of the parameter space Θ for a two-level HAC with two parameters, which is a cone; its origin is indicated by a red point. The blue arrows show the directions used to compute numerical derivatives via finite differences at a given point (in blue): “backward” on the θ_0 -dimension and “forward” on the θ_1 -dimension; see Section 4. (ii, iii) Depiction of the asymptotic local parameter space \mathcal{A} , which equals \mathbb{R}^2 when ϑ is in the interior of Θ (ii), but is a half-space with boundary given by the line $\theta_0 = \theta_1$ when $\vartheta_0 = \vartheta_1$ (iii).

fig:sets1

identity map, thus collapsing the child node into its parent node:

$$C^i = C_i \circ (C^{(i,1)}, \dots, C^{(i,K_i)}) = C_i \circ (C^{(i,1,1)}, \dots, C^{(i,1,K_{(i,1)})}, C^{(i,2)}, \dots, C^{(i,K_i)}),$$

where, on the right-hand side of the equation, C_i is now a $(K_i + K_{(i,1)} - 1)$ -variate function. This is depicted in Figure 1. In view of this, structural hypotheses about HACs can be formulated in terms of equalities between parameters, but these equalities (partially) characterize the boundary of the parameter space, which violates the standard assumptions on the parameter space for inference.

This last concern is intimately related with the more general, and extensively studied problem of determining an appropriate HAC structure from data alone; see Okhrin et al. (2013); Segers and Uyttendaele (2014); Matsypura et al. (2016); Górecki et al. (2017b); Uyttendaele (2018); Okhrin and Ristig (2024) for specific algorithms, and Górecki et al. (2017a) for a review of methods based on Kendall’s tau. Hypothesis testing offers an attractive framework for collapsing nodes, and it can play an important part in structure learning methods. This is made explicit in Segers and Uyttendaele (2014), which uses hypothesis tests based on Kendall distributions (Genest and Rivest, 1993; Nelsen et al., 2003) as part of their structure learning algorithm, and to some extent by (Perreault, 2020, Chapter 3), which discusses structure learning for hierarchical models based on structural hypothesis tests for rank correlations developed in Perreault et al. (2023).

In addition to these theoretical considerations, the constrained parameter space Θ and the difficulty of working with HAC densities give rise to some computational and inferential challenges for the practical usage of HACs (discussed for example in Section 5.1 of Savu and Trede (2010) and Section 4 of Okhrin et al. (2013)). One such challenge is that common numerical optimization techniques for maximizing the log-likelihood may yield a local maximum rather than a global one. To alleviate this problem, Okhrin et al. (2013) proposed a multi-stage estimation procedure, in which parameters are estimated sequentially, starting from the lower levels then upward and treating previously estimated parameters as fixed. We explore the asymptotic behaviour of the

MLEs in fixed dimensions where local maxima are less of a concern and we therefore assume we have access to the MLEs.

1.2 Objectives and paper organization

To provide insight into the uncertainty related to node collapse for overparametrized HACs, we consider the node collapse problem from the perspective of hypothesis testing. Formally, let \mathcal{U}_n be a sample of n observations from a HAC $C = C_{\boldsymbol{\vartheta}}$ given by (3) with one-parameter ∞ -monotone generators of a unique type and Θ of the form (4). We consider hypotheses of the kind

$$H_o : \boldsymbol{\vartheta} \in \Theta_o \quad \text{against} \quad H_{\bullet} : \boldsymbol{\vartheta} \in \Theta, \quad (5) \quad \text{eq:H}$$

where Θ_o is created by taking unions and intersections of subspaces defined by $\Theta_{(\mathbf{i},k)} := \{\boldsymbol{\theta} \in \Theta : \theta_{(\mathbf{i},k)} = \theta_{\mathbf{i}}\}$. Of particular interest are cases when $\Theta_o = \Theta_{\mathbf{i}}$ for some \mathbf{i} (single node collapse), $\Theta_o = \bigcap_{k=1}^{K_{\mathbf{i}}} \Theta_{(\mathbf{i},k)}$ (collapsing all children of node \mathbf{i}), and $\Theta_o = \bigcup_{k=1}^{K_{\mathbf{i}}} \Theta_{(\mathbf{i},k)}$ (collapsing at least one child of node \mathbf{i}).

Our main result provides approximate p -values for the likelihood ratio test of H_o against H_{\bullet} . Specifically, we derive the asymptotic null distribution as $n \rightarrow \infty$ of the test statistic given by

$$L_n := 2\{\ell_n(\hat{\boldsymbol{\theta}}_{\bullet}) - \ell_n(\hat{\boldsymbol{\theta}}_o)\}, \quad \text{where } \ell_n(\boldsymbol{\theta}) = \sum_{\mathbf{u} \in \mathcal{U}_n} \ln c_{\boldsymbol{\theta}}(\mathbf{u}), \quad (6) \quad \text{eq:stat}$$

where $c_{\boldsymbol{\theta}}$ is the copula density associated with $C_{\boldsymbol{\theta}}$, and $\hat{\boldsymbol{\theta}}_o$ and $\hat{\boldsymbol{\theta}}_{\bullet}$ are the (constrained) maximum likelihood estimators of $\boldsymbol{\vartheta}$ under H_o and H_{\bullet} , respectively. Due to overparametrization, the limiting distribution is not the usual χ^2 , it is now mixture distribution whose parameters depend heavily on the underlying space. In practice, it may be difficult to find the asymptotic null distribution, as it involves weights which may not be known apriori. Our focus is to give intuition on behavior of the type-I error control and the power of the test under different configurations of the parameter space, which relates to the tree structure of the overparametrized model. In addition to tests based on the asymptotic distribution of L_n , we consider so-called *conditional* tests, as discussed by (Susko, 2013). When applicable, these are usually much easier to perform than the unconditional tests, although they are in general conservative, see Section 3.4.

As a secondary contribution, we derive analytical formulas for computing the score and the Hessian (or Fisher information) matrix for two-level Clayton and Gumbel HACs, and we investigate analogous numerical methods for approximating these quantities for general HACs. While the analytical formulas may prove useful for future computational or theoretical works, as the score function and the Hessian are often needed for optimization purposes or for deriving the properties of maximum likelihood estimators, their primary purpose here is to help quantifying the effect of numerical error on p -value approximations.

The paper is organized as follows. In §2, we discuss our theoretical framework. In §3, we present our main result and derive tests for H_o from it. We further discuss power under local alternatives, nuisance parameters and a conditional versions of the test. In §4, provide numerical methods for estimating the Fisher information matrix required for these tests; we briefly explain how to derive analytical estimates for two-level hierarchical Clayton or Gumbel copulas in Appendix B.

We investigate the performance of the proposed test in simulations in §5. Specifically, we assess the power and size of the tests in finite sample settings as well as under local alternatives. We conclude the paper in §6 by discussing the implications of our work for structure learning, focusing on the popular algorithm of Okhrin et al. (2013), as well as the newly proposed, and promising algorithm of Okhrin and Ristig (2024) based on penalized estimation. The proofs of our results are presented in Appendix A of the main document, while the additional appendices referred to throughout (Appendices B–E) are available as online supplementary material.

Throughout, we use $\mathcal{N}(\boldsymbol{\mu}, \mathbf{S})$ to denote a Gaussian distribution with mean $\boldsymbol{\mu}$ and covariance \mathbf{S} , $\mathcal{M}(m, \boldsymbol{\gamma})$ to denote a multinomial distribution for m trials with $|\boldsymbol{\gamma}|$ possible results whose probabilities are given by $\boldsymbol{\gamma}$, and $\mathcal{B}(\gamma)$ to denote a Bernoulli distribution with parameter γ .

2 Assumptions

Throughout the paper, we use the following set of assumptions. Assumptions A reformulate and extend the theoretical framework discussed in §1. It ensures that the nesting of the Archimedean copulas produces a valid HAC.

Assumptions A. Let p and d be integers and $\mathcal{C}_{\Theta} = \{C_{\boldsymbol{\theta}} : \boldsymbol{\theta} \in \Theta\}$ be a family of d -variate HACs defined recursively by (3) with $\Theta \subset \mathbb{R}^p$ as in (4), and generated by one-parameter, completely monotone generators of a unique type. Also let \mathcal{U}_n be a dataset of n independent observations from the copula $C_{\boldsymbol{\vartheta}} \in \mathcal{C}_{\Theta}$ and further assume that $\boldsymbol{\vartheta}$ is in the interior of Θ^p , where $\Theta \subseteq [0, \infty)$ is the Archimedean parameter space defined below (4). We use $\boldsymbol{\vartheta}$ for a fixed true value of the parameter, while we use $\boldsymbol{\theta}$ to mean a value of the parameter which may be distinct from $\boldsymbol{\vartheta}$.

The requirement that the HAC be generated from a single family could be relaxed, although, as discussed in the introduction, it is in general difficult to derive the parameter constraints ensuring that 3 defines a proper copula. Additionally some general formulations may prevent the possibility of node collapsing. The assumption $\Theta \subseteq [0, \infty)$, which restricts us to positive dependence, covers most popular HACs. For example, the parameter space of all ten generators in Table 2.2 of Hofert (2010) is either $[0, 1)$, $(0, \infty)$ or $[1, \infty)$.

In addition to Assumptions A, we make the following usual regularity assumptions on the data generating model. They are in general mild, although often difficult to check.

Assumptions B. Assume that under the null, as $n \rightarrow \infty$, the MLEs $\hat{\boldsymbol{\theta}}_{\circ}$ and $\hat{\boldsymbol{\theta}}_{\bullet}$ are consistent estimators of $\boldsymbol{\vartheta}$, and that the local parameter spaces $\mathcal{A}_n := \sqrt{n}(\Theta - \boldsymbol{\vartheta})$ and $\mathcal{A}_{\circ n} := \sqrt{n}(\Theta_{\circ} - \boldsymbol{\vartheta})$ converges to sets \mathcal{A} and \mathcal{A}_{\circ} , respectively. Also assume that the log-likelihood function $\ell_n(\boldsymbol{\theta})$ is differentiable in quadratic mean in a neighbourhood of $\boldsymbol{\vartheta}$ with non-singular Fisher information matrix, and that for every $\boldsymbol{\theta}_1$ and $\boldsymbol{\theta}_2$ in a neighbourhood of $\boldsymbol{\vartheta}$,

$$|\ln c_{\boldsymbol{\theta}_1}(u) - \ln c_{\boldsymbol{\theta}_2}(u)| \leq l'(u) \|\boldsymbol{\theta}_1 - \boldsymbol{\theta}_2\|_2$$

for some function $l' : [0, 1]^d \rightarrow \mathbb{R}$ such that $\mathbb{E}_{\boldsymbol{\vartheta}}\{l'(\mathbf{U})^2\} < \infty$, where $\|\cdot\|_2$ denotes the Euclidean norm.

The local parameter spaces are obtained by centering and rescaling around ϑ in Θ and Θ_{\circ} . Consider for example a two-level HAC with parameter $\vartheta = (\vartheta_0, \vartheta_1)$ and the hypothesis $H_{\circ} : \vartheta_0 = \vartheta_1$. Figure 2.i shows Θ (in turquoise) and Θ_{\circ} (the line $\vartheta_0 = \vartheta_1$). When ϑ is in the interior of Θ , $\mathcal{A} = \mathbb{R}^2$, but when $\vartheta \in \Theta_{\circ}$ (Figure 2.ii), then \mathcal{A} is a half plane (Figure 2.iii). Similarly, $\mathcal{A}_{\circ} = \{(x, x) : x \in \mathbb{R}\}$, provided that $\vartheta \in \Theta_{\circ}$.

Concerning the consistency of the constrained maximum likelihood estimators, recall that we assume (in Assumptions A) that each component of the true parameter ϑ lies in the interior of Θ . This condition, along with others, is often used to ensure consistency; see, *e.g.*, Assumption 1 (ii) in Okhrin and Ristig (2024). For estimation purposes, we use the (full maximum likelihood estimation) algorithm available in the HAC package (Okhrin and Ristig, 2014) in R, which is based on numerical optimization. While such method does not guarantee that the estimators are indeed global maximizers, in practice one can repeat the estimation procedure with several different starting values to maximize the probability of finding the global maximizers. Thus, to limit the scope of the paper, we assume that our MLEs are indeed global maxima, and we point to the works of Geyer (1994) and Shapiro (2000) for extensions to potentially local MLEs.

The good asymptotic behaviour of the local parameter spaces is perhaps the easiest condition to check. As we will see in §3, all the specific structural hypotheses we consider lead to local spaces converging to cones: sets $\mathcal{C} \subseteq \mathbb{R}^p$ such that $\mathbf{x} \in \mathcal{C}$ if and only if $\lambda \mathbf{x} \in \mathcal{C}$ for all $\lambda \geq 0$. The existence of such cones is often referred to as Chernoff regularity, due to their use by the latter in his seminal work Chernoff (1954) on inference under non-standard conditions. The exact shape of these cones has a significant impact on the limiting null distributions of our tests.

The differentiability in quadratic mean (DQM) of the log-likelihood and the non-singularity of the Fisher information matrix at the true parameter are standard conditions in the asymptotics literature; the latter condition is difficult to check due to generally cumbersome (even for very shallow HACs) differentiation formulas. Fortunately, the invertibility condition can, to some extent, be checked numerically. In particular, non-invertibility of the Fisher information matrix is usually flagged during estimation steps, as it generally leads to computational issues during numerical optimization. The DQM condition is satisfied if the likelihood is second-order continuously differentiable, but we note the DQM condition alone may not be sufficient to guarantee the good performance of numerical procedures needed to estimate the Fisher information matrix. To guarantee numerical convergence of finite difference methods which we employ, it is sufficient to have an additional order of smoothness, for example to numerically estimate the second-order derivative it is sufficient to require smoothness on the third-order derivative. Luckily, most models used in practice are very smooth with most being infinitely differentiable functions. These assumptions are the analogous versions of Assumptions 2 (i) and 3 in Okhrin and Ristig (2024).

Finally the Lipschitz assumption on the log-likelihood function is standard in the analysis of parametric models, see (van der Vaart, 1998, Chapter 5), and may be further weakened to an assumption bracketing number on the log-likelihood (van der Vaart, 1998, Theorem 19.4). This particular assumption is not as often used in the HAC literature, so we verify this for a two-level Clayton HAC, showing that these assumptions can be satisfied in practice; indeed most smooth parametric families of Archimedean copulas should satisfy these requirements. This Assumption is

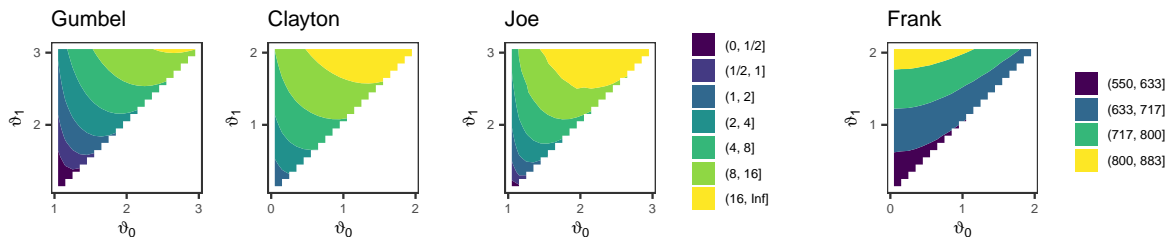


Figure 3: Numerical approximation of the determinant of Σ for Clayton and Gumbel trivariate HACs with trivial structure $\mathcal{G} = \{\{1, 2\}, 3\}$, as a function of their parameters $\vartheta = (\vartheta_0, \vartheta_1)$. It is computed on a grid in a neighborhood of the origin $\mathbf{o} = (o, o)$ of the cone Θ ; $o = 1$ for Gumbel and Joe generators and $o = 0$ for Clayton and Frank generators. Note that the vertical boundary $\{o\} \times \Theta$ is part of Θ only if $o \in \Theta$, but the oblique boundary $\{(\vartheta, \vartheta) : \vartheta \in \Theta\}$ always is. All values on this grid are positive, meaning that Σ is invertible.

determinant

similar to Assumption 2 (ii) in Okhrin and Ristig (2024), as they are both used to invoke a uniform strong law of large numbers needed to prove the asymptotic normality of the MLE.

For an example of how Assumptions B can be verified in practice for a simple Clayton HAC, see Appendix C. The only condition not verified is the invertibility of the Fisher information matrix which we provide some numerical evidence for in Figure 3.

3 Likelihood ratio tests

sec:tests

We are now ready to investigate the asymptotic behavior of the MLE and the likelihood ratio L_n for testing hypotheses H_o against H_\bullet , as defined by (4) and (5). Specifically, we provide an asymptotic stochastic representation for L_n , which we then use to derive explicit distributions in some special cases. We also discuss handling nuisance parameters as well as an alternative method for approximating the null distribution of L_n that is computationally simpler, but which might be overly conservative in certain cases. Note that for practical purposes, one could exploit available sampling algorithms for HACs (Whelan, 2004; McNeil, 2008; Hofert, 2010, 2011; Hofert and Mächler, 2011; Okhrin and Ristig, 2014; Grothe and Hofert, 2015; Górecki et al., 2021; Hofert et al., 2023) to approximate the null distribution of L_n by generating new datasets from the HAC with parameter $\hat{\theta}_o$ and computing the associated value of L_n for each of them. However this requires repeated numerical optimizations and is computationally demanding even for moderately large parameter spaces.

3.1 Test via the asymptotic null distribution of L_n

-asymptotic

As it will be useful later on, we consider local alternatives characterized by a deviation parameter $\mathbf{h} \in \mathbb{R}^p$; results under the null are obtained by setting $\mathbf{h} = \mathbf{0}$. Our main result involves a p -dimensional random vector $\mathbf{Z} \sim \mathcal{N}(\mathbf{h}, \Sigma)$, with Σ as in Assumptions B, and its projections onto

the sets \mathcal{A} and \mathcal{A}_\circ , based on the squared Σ -Mahalanobis distance:

$$\mathbf{Z}_\bullet := \inf_{z \in \mathcal{A}} q_{\mathbf{Z}}(z) \quad \text{and} \quad \mathbf{Z}_\circ := \inf_{z \in \mathcal{A}_\circ} q_{\mathbf{Z}}(z), \quad q_{\mathbf{Z}}(z) = (\mathbf{Z} - z)^\top \Sigma^{-1} (\mathbf{Z} - z). \quad (7)$$

In practice, when $\mathbf{Z} \notin \Theta$, we compute \mathbf{Z}_\bullet by projecting \mathbf{Z} onto all faces of \mathcal{A} and selecting the optimal one; \mathbf{Z}_\circ is computed similarly. The following theorem, which provides an asymptotic stochastic representation for L_n , is a consequence of Theorem 16.7 of van der Vaart (1998).

Theorem 1. *Under Assumptions A and B, let $\hat{\theta}_\circ$ and $\hat{\theta}_\bullet$ be the maximum likelihood estimators of $\vartheta'_n = \vartheta + \mathbf{h}_n/\sqrt{n}$ ($\mathbf{h}_n \rightarrow \mathbf{h} \in \mathbb{R}^p$ as $n \rightarrow \infty$) over Θ_\circ and Θ , respectively, and for $\mathbf{Z} \sim \mathcal{N}(\mathbf{h}, \Sigma)$, let \mathbf{Z}_\bullet , \mathbf{Z}_\circ , and $q_{\mathbf{Z}}$ be as in (7). Then \mathbf{Z}_\circ and \mathbf{Z}_\bullet are unique for almost all \mathbf{Z} and*

$$\sqrt{n}(\hat{\theta}_\bullet - \hat{\theta}_\circ) \rightsquigarrow \mathbf{Z}_\bullet - \mathbf{Z}_\circ \quad \text{and} \quad L_n \rightsquigarrow L_\infty := q_{\mathbf{Z}}(\mathbf{Z}_\circ) - q_{\mathbf{Z}}(\mathbf{Z}_\bullet) \quad \text{as } n \rightarrow \infty, \quad (8)$$

where \rightsquigarrow denotes convergence in distribution.

Theorem 1 provides asymptotic stochastic representations not only for L_n , but for many other popular test statistics via the continuous mapping Theorem, most notably for Wald-type statistics. When Σ is unknown, as is often the case, Theorem 1 remains valid when Σ is replaced with a consistent estimator $\hat{\Sigma}$, by Slutsky's Lemma. We provide such an estimator in §4.

Given a consistent estimate $\hat{\Sigma}$ of Σ , a p -value for testing H_\circ against H_\bullet can be obtained by approximating the distribution of L_n using Monte Carlo replicates based on $\mathbf{Z} \sim \mathcal{N}(\mathbf{0}, \hat{\Sigma})$, following (7) and (8). Alternatively, one can try to refine Theorem 1, following for example Bartholomew (1959a,b, 1961); Kudo (1963); Moran (1971); Chant (1974); Shapiro (1985); Self and Liang (1987). In particular, it can be shown that, under certain conditions, the distribution of L_∞ is a mixture of independent chi-squared distributions, often referred to as a $\bar{\chi}^2$ distribution. To derive such refinements, we make use of the following lemma, adapted from Shapiro (1985, Lemma 3.1).

Lemma 1. *Let $\mathbf{Z} \sim \mathcal{N}(\mathbf{0}, \Sigma)$ for some positive definite matrix Σ and \mathcal{C} be the cone defined by $\mathcal{C} = \{\mathbf{z} \in \mathbb{R}^p : \mathbf{x}_k^\top \mathbf{z} \leq 0, k = 1, \dots, p\}$ for some fixed vectors $\{\mathbf{x}_k\}_{k=1}^p$. Further suppose that there exists \mathbf{P}_\circ and \mathbf{P}_\bullet such that the following holds: $\mathbf{Z}_\circ = \mathbf{P}_\circ \mathbf{Z}$ and $\mathbf{Z}_\bullet = \mathbf{P}_\bullet \mathbf{Z}$ whenever $\mathbf{Z} \in \mathcal{C}$; $\mathbf{P} := \mathbf{P}_\bullet - \mathbf{P}_\circ$ is a matrix of rank ν such that $\Sigma^{1/2} \mathbf{P}^\top \Sigma^{-1} \mathbf{P} \Sigma^{1/2}$ is idempotent; and $\mathbf{P} \mathbf{x}_k \in \{\mathbf{0}, \mathbf{x}_k\}$ for each $k \in \{1, \dots, p\}$. Then, $(L_\infty | \mathbf{Z} \in \mathcal{C}) \sim \chi_\nu^2$.*

To give a general idea of what the asymptotic distribution of the likelihood ratio test look like in practice we now consider some simple HACs. Generally the mixture weights will depend on Σ , but we begin with an example in which L_∞ follows a $\bar{\chi}^2$ distribution with mixture weights that do not depend on Σ . It concerns two-level HACs with only two non-leaf nodes, which, in the notation of (3), corresponds to the case $K_{(0)} \geq 2$, $d_{(0,1)} \geq 2$ and $d_{(0,k)} = 1$, for $2 \leq k \leq K_{(0)}$.

Corollary 1. *Suppose that C_ϑ is a two-level HAC with parameter $\vartheta = (\vartheta_0, \vartheta_1)$, then under the assumptions of Theorem 1 and $H_\circ : \vartheta_0 = \vartheta_1$ ($\Theta_\circ = \Theta_{(0,1)}$), $L_\infty \sim W_1 \chi_1^2$, with $W_1 \sim \mathcal{B}(1/2)$.*

The following corollaries treat a similar case, the only difference being that the root node contains two twin non-leaf children; $K_{(0)} \geq 2$, $d_{(0,1)} = d_{(0,2)} \geq 2$ and $d_{(0,k)} = 1$ ($2 < k \leq K_{(0)}$) in

(3). They respectively concern intersection and union hypotheses. Note that the mixture weights depends on Σ this time.

cor:simple-2

Corollary 2. *Suppose that $C_{\mathfrak{g}}$ is a two-level HAC with parameter $\vartheta = (\vartheta_0, \vartheta_1, \vartheta_2)$, let \mathbf{Z} be the Gaussian vector given in Theorem 1 with $\sigma_k^2 = \text{Var}(Z_k)$, and $\sigma_{k,k+1} = \text{Cov}(Z_k, Z_{k+1})$ for $k = 0, 1$. Then, under the assumptions of Theorem 1 and $H_o : \vartheta_0 = \vartheta_1 = \vartheta_2$ ($\Theta_o = \Theta_{(0,1)} \cap \Theta_{(0,2)}$),*

$$L_\infty \sim W_1\chi_1^2 + W_2\chi_2^2, \quad \text{for some } (W_0, W_1, W_2) \sim \mathcal{M}\{1, (\gamma_0, \gamma_1, \gamma_2)\},$$

where $\gamma_0 = \cos^{-1}(\beta)/(2\pi)$, $\gamma_1 = 1/2$ and $\gamma_2 = 1/2 - \gamma_0$ with $\beta = (\sigma_0^2 - 2\sigma_{01} + \sigma_{12})/(\sigma_0^2 - 2\sigma_{01} + \sigma_1^2)$.

cor:simple-3

Corollary 3. *Suppose that $C_{\mathfrak{g}}$ is a two-level HAC with parameter $\vartheta = (\vartheta_0, \vartheta_1, \vartheta_2)$ and let $W_1 \sim \mathcal{B}(1/2)$, then under the assumptions of Theorem 1 and $H_o : \vartheta_0 \in \{\vartheta_1, \vartheta_2\}$ ($\Theta_o = \Theta_{(0,1)} \cup \Theta_{(0,2)}$), $L_\infty \preceq W_1\chi_1^2$ if $\vartheta_1 = \vartheta_2$, where \preceq denotes stochastic dominance, and $L_\infty \sim W_1\chi_1^2$ otherwise.*

In this latter case, it is not specified by the null whether only one of or both ϑ_1 and ϑ_2 equal ϑ_0 . The distribution of L_∞ is thus unknown, but one can ensure that the corresponding test is asymptotically conservative, at worst, by using $W_1\chi_1^2$ as the reference distribution for L_n .

power-local

3.2 Power under local alternatives

Fix an Archimedean generator family and suppose that ϑ satisfies some hypothesis H_o of interest. To investigate the asymptotic properties of the likelihood ratio test of §3.1, one can define local departures from H_o by setting some entries of \mathbf{h} to non-zero values in Theorem 1 and studying the asymptotic distribution of L_n in these cases. Specifically, when \mathbf{h} depends only on a scalar h , one can produce so-called power curves by recording the power of the test at some given nominal level α for each value of h .

As an example, consider testing $H_o : \vartheta_0 = \vartheta_1$ against H_\bullet of (5) in the HAC of Corollary 1, when the parameter generating the data is given by $\vartheta + \mathbf{h}_n/\sqrt{n}$, where $\vartheta = (\vartheta, \vartheta)$ for some $\vartheta \in \Theta$ and $\mathbf{h}_n \rightarrow \mathbf{h}$ as $n \rightarrow \infty$. To allow for a meaningful comparison across families we set the local parameter \mathbf{h}_n so that it corresponds to a specific discrepancy in Kendall's τ ; this is desirable as Kendall's τ has a universal interpretation not linked to any specific parametrization of the copula. We can do this by exploiting the bijective relationship between the parameter ϑ and Kendall's τ in bivariate Archimedean copulas. More precisely, for a given generator ψ and a given discrepancy h' on the τ scale, we set

$$\mathbf{h}_n := \sqrt{n}\{\tau_\psi^{-1}(\tau_\psi(\vartheta) + h'e/\sqrt{n}) - \vartheta\}, \quad \text{with } \mathbf{e} := (e_0, e_1) \text{ such that } e_1 - e_0 = 1,$$

where $\tau_\psi : \Theta \rightarrow [0, 1]$ is the family-specific function that returns the Kendall correlation corresponding to ϑ ; see Table 2.2 in Hofert (2010) for analytical expressions of τ_ψ for a variety of families and the `copula` package in R Hofert et al. (2023) for implementations of τ_ψ and τ_ψ^{-1} . One can check that for Gumbel, Clayton, Frank and Joe generators, $\mathbf{h} = h\mathbf{e}$ for some h ; in particular, $h = h'/(1 - \tau)^2$ for the Gumbel family and $h = 2h'/(1 - \tau)^2$ for the Clayton, where $\tau = \tau_\psi(\vartheta)$.

Remark 1. The local power of the test is invariant to the choice of \mathbf{e} , as the constraint $e_1 - e_0 = 1$ ensures that \mathbf{h} lies on a line parallel to the local null space $\mathcal{A}_o = \{(z_0, z_1) : z_0 = z_1\}$.

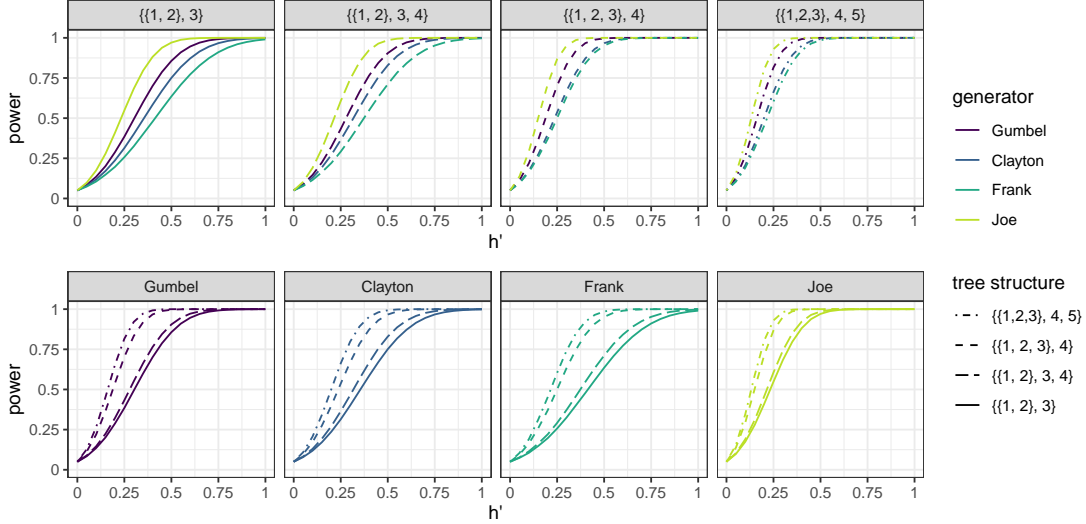


Figure 4: Power curves at nominal level $\alpha = 0.05$ for tests of $H_o : \vartheta_0 = \vartheta_1$ against $H_\bullet : (\vartheta, \vartheta) + \mathbf{h}_n/\sqrt{n}$, when $\vartheta = \tau_\psi^{-1}(1/3)$. Four generator families (Gumbel, Clayton, Frank and Joe) and four two-parameter structures are considered, for a total of sixteen distinct distributions. The top and bottom panels show the same results from a different perspective: the top panels compare the local power across the families for a given tree structure, while the bottom panels compare the local power across tree structures for a given family.

power-curves

For a given nominal level α and a given generator family, the resulting power curve takes the form $\beta_\alpha(h') := \mathbb{P}\{L > c_\alpha\}$, where c_α is the $(1 - 2\alpha)$ th quantile of the χ_1^2 distribution. We compute this latter using Monte Carlo replicates of $\mathbf{Z} \sim \mathcal{N}(\mathbf{h}, \tilde{\Sigma})$, where $\tilde{\Sigma}$ is an estimator of Σ based on a very large dataset generated from the null HAC model. Note that Monte Carlo sampling of \mathbf{Z} is not required to compute $\mathbb{P}(L = 0)$, since $\mathbb{P}(L = 0) = \Phi(0)$, where Φ is the normal cumulative distribution function with mean parameter $h_1 - h_0$ ($\mathbf{h} = (h_0, h_1)$) and variance parameter $\sigma_0^2 + \sigma_1^2 - 2\sigma_{01}$ (in the notation of Corollary 2).

Figure 4 shows the power curves, computed at nominal level $\alpha = 0.05$, for Gumbel, Clayton, Frank and Joe HACs and four distinct structures involving two parameters. The top panels highlight the difference in performance across the families. For each structure considered, the test performed best for the Joe case, followed by the Gumbel, Clayton, and then Frank cases. The bottom panels, which show the same results from a different perspective, highlight the fact that power increases with the number of variables.

3.3 Nuisance parameters

ec:nuisance

We now consider cases where the parameter vector of interest, constrained by H_o , is a sub-vector of ϑ , so that the latter contains so-called nuisance parameters. For convenience, we assume that the parameters of interest, say $(\vartheta_i)_{i \in \mathcal{I}'}$ for some $\mathcal{I}' \subset \mathcal{I}$, are such that the nodes indexed by \mathcal{I}' corresponds to a contiguous sub-tree of the HAC. Without loss of generality, we further assume that \mathcal{I}' contains the root node; otherwise one could get rid of some nuisance parameters by working

directly with the margin C^j for which $j = \arg \min_{\mathbf{i} \in \mathcal{I}'} |\mathbf{i}|$, as defined in 3.

We first discuss cases assuming all nuisance parameters, say $\vartheta_{(i,k)}$, are distinct from their respective neighboring parameters, i.e., $\vartheta_i < \vartheta_{(i,k)} < \vartheta_{(i,k,r)}$ for all $r \in \{1, \dots, K_{(i,k)}\}$. Aside from the extra variation they might induce in the estimation procedure, such parameters do not affect the application of Theorem 1, as the dimensions in \mathcal{A}_\bullet and \mathcal{A}_\circ to which they correspond then all coincide with \mathbb{R} . This is exemplified in the following corollary dealing with a case similar to Corollary 1 but with an additional nuisance parameter, and for which we recover the same limiting distribution for L_n ; its proof follows from that of Corollary 3.

cor:nuisance

Corollary 4. *Suppose that C_ϑ is a two-level HAC with parameter $\vartheta = (\vartheta_0, \vartheta_1, \vartheta_2)$ such that $\vartheta_1 < \vartheta_2$, then under the assumptions of Theorem 1 and $H_\circ : \vartheta_0 = \vartheta_1$ ($\Theta_\circ = \Theta_{(0,1)}$), $L_\infty \sim W_1 \chi_1^2$, where $W_1 \sim \mathcal{B}(1/2)$.*

A more serious challenge arises when it is not clear whether the nuisance parameters are distinct from their neighboring parameters or not, thus creating some uncertainty as to exactly which alternative hypothesis $H_\bullet : \vartheta \in \Theta_\bullet$ (with $\Theta_\bullet \subseteq \Theta$) to use. Since different choices of alternative hypothesis lead to a different null space Θ_\circ and in turn different local spaces \mathcal{A} and \mathcal{A}_\circ , this creates the possibility of a mismatch between the limiting distribution used and the true distribution of L_∞ . For example, we derive the distribution of L_∞ in a case similar to Corollary 4, this time with all parameters being equal.

nuisance-2

Corollary 5. *Suppose that C_ϑ is two-level HAC with parameter $\vartheta = (\vartheta_0, \vartheta_1, \vartheta_2)$ such that $\vartheta_0 = \vartheta_1 = \vartheta_2$, let \mathbf{Z} be the Gaussian vector given in Theorem 1, $\sigma_k^2 = \text{Var}(Z_k)$ and $\sigma_{k,k+1} = \text{Cov}(Z_k, Z_{k+1})$ for $k = 0, 1$. Further let $\beta = (\sigma_0^2 - 2\sigma_{01} + \sigma_{12}) / (\sigma_0^2 - 2\sigma_{01} + \sigma_1^2)$ and assume that $\beta \geq 0$. Then, under the assumptions of Theorem 1 and $H_\circ : \vartheta_0 = \vartheta_1$ ($\Theta_\circ = \Theta_{(0,1)}$),*

$$L_\infty \sim W_1 \chi_1^2 + W_2 \chi_2^2, \quad \text{for some } (W_0, W_1, W_2) \sim \mathcal{M}\{1, (\gamma_0'', \gamma_1'', \gamma_2'')\},$$

where $\gamma_0'' = 1/4 + \cos^{-1}(\beta)/(2\pi)$, $\gamma_1'' = 1/2$ and $\gamma_2'' = 1/2 - \gamma_0''$.

Naturally, if one knew that $\vartheta_0 = \vartheta_2$, one would eliminate ϑ_2 by collapsing the HAC and then relying on Corollary 1 for inference. Corollary 5 shows that the cost of keeping ϑ_2 in the model is extra noise in the form of an additional χ_2^2 component. On the other hand, we see by comparing Corollaries 4 and 5 that for such two-level HACs ($\beta > 0$) with $\vartheta_0 = \vartheta_2$, keeping both parameters in the model leads to a conservative test. Furthermore, the two tests are equivalent when $\beta = 0$.

Extensions to two-level structures with more nuisance parameters sharing the same value should be relatively simple. In more complex cases involving, say, q nuisance parameters with unclear status, a simple strategy is to repeat the test for all 2^q candidate sets Θ_\bullet obtained by setting each of them either equal to their closest neighbour (and collapsing the HAC) or not, and then combine or summarize the observed p -values. In particular, using the largest of the p -values thus obtained guarantees that the test is at worst conservative, although for large q we expect this to perform poorly.

rem:hybrid

Remark 2. When q is large, one might instead compute a single p -value using a hybrid null distribution. To illustrate the idea, consider again testing $H_\circ : \vartheta_0 = \vartheta_1$ against $H_\bullet : \vartheta_0 < \vartheta_1$ in

the presence of a nuisance parameter ϑ_2 , as in Corollaries 4 and 5, and let $h_n = \sqrt{n}(\hat{\theta}_{o2} - \hat{\theta}_{o0})$ and $\mathbf{h}_n := (0, 0, h_n)$; in general, \mathbf{h}_n would have q non-zero entries. To test H_o , it seems reasonable to use a null distribution similar to that in Corollary 4 when h_n is large, but similar to that in Corollary 5 when h_n is small. This can be done by setting the mean of \mathbf{Z} in Theorem 1 to \mathbf{h}_n . If $\vartheta_0 < \vartheta_2$ is true, then $h_n \rightarrow \infty$ as $n \rightarrow \infty$ and one eventually recovers the asymptotic null distribution in Corollary 4. If however $\vartheta_0 = \vartheta_2$ is true, then h'_n does not converge to a constant, although $h'_n = 0$ with probability $\sim \gamma_0''$ (as in Corollary 5) for large n . Thus, in this case, one does not exactly recover the asymptotic null distribution in Corollary 5. Yet, it seems reasonable to believe that the distribution thus obtained is a sensible approximation of the unknown true null distribution. See Appendix Figure A.1 for a visual description of the hybrid null distribution. We investigate the specific case discussed above in simulations in §5, and find that the approximation is very accurate in the cases considered.

3.4 A conditional test based on the asymptotic null distribution of L_n

To circumvent the estimation of Σ when testing H_o , one may consider the method discussed by Susko (2013) which is based on (Bartholomew, 1961). The main idea is to partition the space Θ (and, accordingly, \mathcal{A}) into regions (say Θ^ν and \mathcal{A}^ν) for which the distribution of $(L_\infty | \mathbf{Z}_\bullet \in \mathcal{A}^\nu)$ is known, and when $\hat{\theta}_\bullet \in \Theta^\nu$ we base our test on the latter distribution rather than on that of L_∞ . This method is thus particularly useful when L_∞ is a $\bar{\chi}^2$ distribution, as in the case developed in Corollaries 1–5, where $(L_\infty | \mathbf{Z}_\bullet \in \mathcal{A}^\nu) \sim \chi_\nu^2$ and ν is the number of extra constraints introduced by passing from $\hat{\theta}_\bullet$ to $\hat{\theta}_o$. In doing so, however, one should expect generally conservative sizes and some loss in power, although in some special cases it might lead to an increase in power (Susko, 2013, Section 5).

Remark 3. As an example, consider the HAC in Corollary 1, where $\vartheta = (\vartheta_0, \vartheta_1)$ and $H_o : \vartheta_0 = \vartheta_1$. In this case, \mathbf{P}_o is always a matrix of rank 2, and $\mathbf{P}_\bullet = \mathbf{I}$, when $Z_0 < Z_1$, or $\mathbf{P}_\bullet = \mathbf{P}_o$, when $Z_0 > Z_1$. The event $Z_0 = Z_1$ has zero probability. Thus, $(L_n | \hat{\theta}_\bullet \in \Theta^\nu) \rightsquigarrow \chi_\nu^2$, where $\Theta^0 = \Theta_o$ and $\Theta^1 = \{(\theta_0, \theta_1) : \theta_0 < \theta_1\}$. The test rejects H_o only when $\nu = 1$ and $\mathbb{P}(\chi_1^2 > L_n) < \alpha$, where α is the nominal test level. In particular, it has an asymptotic size of $\alpha/2$.

For comparison, consider the HAC in Corollary 2, where $\vartheta = (\vartheta_0, \vartheta_1, \vartheta_2)$, $H_o : \vartheta_0 = \vartheta_1 = \vartheta_2$ and $H_\bullet : \vartheta_0 \leq \vartheta_1, \vartheta_2$. In this case, $\Theta^1 = \cup_{k=0,1} \{\theta : \theta_0 = \theta_{1+k} < \theta_{2-k}\}$ and $\Theta^2 = \{\theta : \theta_0 < \theta_1, \theta_2\}$. The test rejects H_o only when $\nu \in \{1, 2\}$ and $\mathbb{P}(\chi_\nu^2 > L_n) < \alpha$, and therefore, in the notation of Corollary 2, the test has an asymptotic size of $(\gamma_1 + \gamma_2)\alpha > \alpha/2$. This suggests more generally that the asymptotic size of the conditional test in similar situations is $(1 - \gamma_0)\alpha$, where $\gamma_0 = \mathbb{P}(\hat{\theta}_\bullet \in \Theta_o)$. For hypotheses H_o involving many intersections ($\Theta_o = \cap_{\mathcal{I}_o} \Theta_{\mathbf{i}}$ with $|\mathcal{I}_o|$ large), we expect that γ_0 be close to zero and hence that the loss in size be negligible.

The above discussion also suggests that the conditional test can be made asymptotically exact by replacing the desired nominal level α by $\alpha/(1 - \gamma_0)$, although this might require estimating γ_0 . Even in this case, however, the conditional and unconditional tests are still intrinsically different, as they do not use the same critical regions. The conditional test uses a critical value that varies depending on the location of $\hat{\theta}_\bullet$ in Θ , while the unconditional test uses a fixed critical value. This

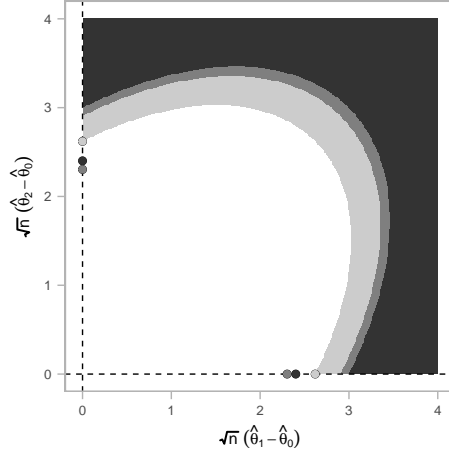


Figure 5: Depiction of the rejection regions associated with the unconditional test based on Theorem 1 (all shades of gray) and the exact (two darkest shade of gray) and conservative (the darkest shade of gray) conditional tests discussed in §3.4 under the setup of Corollary 2 ($H_o : \vartheta_0 = \vartheta_1 = \vartheta_2$) with $\Sigma = \mathbf{I}$. To ease the interpretation, the regions are plotted in terms of the vector $\sqrt{n}(\hat{\theta}_{\bullet 1} - \hat{\theta}_{\bullet 0}, \hat{\theta}_{\bullet 2} - \hat{\theta}_{\bullet 0})$ as opposed to $\sqrt{n}(\boldsymbol{\theta} - \boldsymbol{\vartheta})$; the spaces \mathcal{A} and \mathcal{A}_o are mapped to $[0, \infty) \times [0, \infty)$ and the origin $(0, 0)$, respectively. The points on the x and y axes correspond to the critical values used by the tests when $\hat{\theta}_{\bullet 0} = \hat{\theta}_{\bullet 2}$ and $\hat{\theta}_{\bullet 0} = \hat{\theta}_{\bullet 1}$, respectively.

2-rejection

is depicted in Figure 5, which shows the rejection regions associated with the unconditional and the two conditional tests (the conservative test and the asymptotically exact test) under the setup of Corollary 2 for $\Sigma = \mathbf{I}$. Analogously, one can think of the difference between the conditional and the unconditional tests as coming from their implied long term sampling schemes. The unconditional test proposes that we resample from the data generating distribution, while the conditional tests propose that we sample from data which produces an MLE in the same the region of $\hat{\theta}_{\bullet}$. The loss in size for the conditional method stems from the fact that the null is never rejected when $\hat{\theta}_{\bullet}$ is contained in Θ_o .

4 Estimation of the Fisher information matrix

-estimation

We now turn to the estimation of Σ , which is required in most situations to apply Theorem 1. By the second Bartlett identity, Σ is the inverse of the Fisher Information matrix $\mathbf{I}_{\boldsymbol{\vartheta}} := -\mathbb{E}\{\mathbf{J}_{\boldsymbol{\vartheta}}(\mathbf{U})\}$, where $\mathbf{J}_{\boldsymbol{\vartheta}}(\mathbf{U}) = \partial^2 \ln c_{\boldsymbol{\vartheta}}(\mathbf{U}) / (\partial \boldsymbol{\theta} \partial \boldsymbol{\theta}^{\top})$ evaluated at $\boldsymbol{\theta} = \boldsymbol{\vartheta}$. Since $\mathbf{I}_{\boldsymbol{\vartheta}}$ is often difficult to express explicitly and $\boldsymbol{\vartheta}$ is unknown, Σ is usually estimated from the data $\mathcal{U}_n := \{\mathbf{U}_r\}_{r=1}^n$ as the inverse of $(1/n) \sum_{r=1}^n \mathbf{J}_{\hat{\boldsymbol{\theta}}}(\mathbf{U}_r)$ where $\hat{\boldsymbol{\theta}} \in \{\hat{\boldsymbol{\theta}}_o, \hat{\boldsymbol{\theta}}_{\bullet}\}$. Under weak conditions such as those in Assumptions A–B, this estimator is consistent. In Appendix B, we provide the necessary formulas to compute this estimator for two-level Clayton and Gumbel HACs. But even in these simple cases the complex nature of $c_{\boldsymbol{\vartheta}}$ makes the derivations cumbersome. Therefore we expect that for more complex HACs an additional numerical procedure for estimating Σ would be beneficial, we explore this below.

We consider approximating the second-order partial derivatives by their finite difference analogues; this requires a bit of care to ensure that the log-likelihood is evaluated at points inside the

parameter space. For example, consider two parameters of interest (constrained by H_o) which lie on two consecutive levels and let $\ell_r^*(\boldsymbol{\theta}) := \ln c_{\boldsymbol{\theta}}(\mathbf{U}_r)$ for all $\mathbf{U}_r \in \mathcal{U}_n$. In this case, we use backward differences for the parameter from the higher level, and forward differences for the parameter from the lower level in order to remain in the parameter space; this is depicted Figure 2.i (blue arrows). Concretely, we approximate the off-diagonal entry of $\mathbf{I}_{\boldsymbol{\theta}}$ associated with two nodes \mathbf{i} and (\mathbf{i}, k) with

$$\frac{\partial^2 \ell_r^*(\boldsymbol{\theta})}{\partial \theta_{\mathbf{i}} \partial \theta_{(\mathbf{i}, k)}} \approx D(\boldsymbol{\theta} | \mathbf{U}_r) := \frac{\ell_r^*(\boldsymbol{\theta} + \boldsymbol{\delta}_{(\mathbf{i}, k)}) - \ell_r^*(\boldsymbol{\theta}) - \ell_r^*(\boldsymbol{\theta} - \boldsymbol{\delta}_{\mathbf{i}} + \boldsymbol{\delta}_{(\mathbf{i}, k)}) + \ell_r^*(\boldsymbol{\theta} - \boldsymbol{\delta}_{\mathbf{i}})}{\delta_{\mathbf{i}}^* \delta_{(\mathbf{i}, k)}^*}, \quad (9)$$

eq:finite-d

where for node $\mathbf{j} \in \{\mathbf{i}, (\mathbf{i}, k)\}$, $\boldsymbol{\delta}_{\mathbf{j}}$ is a p -dimensional vector with a single non-zero entry, and $\delta_{\mathbf{j}}^*$ is the (node-specific) value of this latter. The numerical error of this scheme will be negligible in the limit if the third order derivative exists and is bounded in a neighbourhood of the evaluation point; this can be easily argued through a Taylor expansion.

For a given node \mathbf{i} , it is possible that $\ell_r^*(\boldsymbol{\theta} - \boldsymbol{\delta}_{\mathbf{i}})$ varies considerably with respect to small changes in $\theta_{\mathbf{i}}$, leading to unstable behaviour when $\ell_r^*(\boldsymbol{\theta})$ and $\ell_r^*(\boldsymbol{\theta} - \boldsymbol{\delta}_{\mathbf{i}})$ are numerically indistinguishable. To alleviate this problem, we follow a reasoning similar to that of §3.2 and define $\delta_{\mathbf{i}}^*$ so that it corresponds to a small discrepancy of δ^τ in the associated Kendall correlation value; we use $\delta^\tau = 0.005$. Specifically, we let $\delta_{\mathbf{i}}^* = \tau_\psi^{-1}\{\tau_\psi(\theta_{\mathbf{i}}) - \delta^\tau\} - \theta_{\mathbf{i}}$, where $\tau_\psi(\theta)$ is the family-specific function that returns the Kendall correlation corresponding to the Archimedean parameter θ , and we proceed similarly for $\delta_{(\mathbf{i}, k)}^*$.

More general hypotheses for equality of parameters from adjacent nodes on three or more levels, say $H_o : \vartheta_{(0)} = \vartheta_{(0,1)} = \vartheta_{(0,1,1)}$, is more complex. This is because the estimate $\hat{\theta}_{o(0,1)}$ must satisfy $\hat{\theta}_{o(0)} \leq \hat{\theta}_{o(0,1)} \leq \hat{\theta}_{o(0,1,1)}$, leaving no space around it to compute numerical derivatives. In such cases, one can further exploit Theorem 1 and replace the subvector $(\hat{\theta}_{o(0)}, \hat{\theta}_{o(0,1)}, \hat{\theta}_{o(0,1,1)})$ of the null-constrained MLE by $(\hat{\theta}_{o(0)}, \hat{\theta}_{o(0,1)}, \hat{\theta}_{o(0,1,1)}) + (-\delta_{(0)}^*, 0, \delta_{(0,1,1)}^*)g(n)$, where $g(n)$ is $O(1/\sqrt{n})$. The hypothesized parameter, which satisfies a specific local alternative to H_o , now lies in the interior of $\boldsymbol{\Theta}$, allowing the use of central finite differences to approximate the partial derivatives, while leaving $\boldsymbol{\Sigma}$ invariant. Other cases can be handled similarly by choosing a suitable local deviation from the null.

In addition to the estimator of $\mathbf{I}_{\boldsymbol{\theta}}$ just described, that is, $(1/n) \sum_{i=1}^n D(\hat{\boldsymbol{\theta}} | \mathbf{U}_i)$ with D a finite difference scheme such as that in (9) and $\hat{\boldsymbol{\theta}} \in \{\hat{\boldsymbol{\theta}}_o, \hat{\boldsymbol{\theta}}_\bullet\}$, we investigate a second approach based on Monte Carlo replicates. Specifically, we propose to exploit known sampling algorithms for HACs (e.g., from the HAC package Okhrin and Ristig (2014)) to approximate the expectation $\mathbb{E}D(\hat{\boldsymbol{\theta}} | \mathbf{U}) \approx \mathbf{I}_{\boldsymbol{\theta}}$ with $(1/N) \sum_{i=1}^N D(\hat{\boldsymbol{\theta}} | \mathbf{U}'_i)$, where N is a large integer and $\{\mathbf{U}'_i\}_{i=1}^N$ are Monte Carlo replicates from $C_{\hat{\boldsymbol{\theta}}}$. Simulations involving minimal two-parameter Gumbel and Clayton HACs show that the use of Monte Carlo sampling can significantly reduce the estimation noise for small sample sizes. This can be seen in Figure 6, which provides boxplots of the results for the estimation of $\Sigma_{00} := \text{Var}(Z_0)$ for Clayton HACs in a simple scenario, and in Appendix Figure D.1, which shows the results for all entries of $\boldsymbol{\Sigma}$ and for both families in the same scenario. The results also suggest that the finite difference approximation is very accurate and that, when the null is true, the use of $\hat{\boldsymbol{\theta}} = \hat{\boldsymbol{\theta}}_\bullet$ introduces a bias for small sample sizes. For large sample sizes, the estimators based on the observed and Monte Carlo data both perform well.

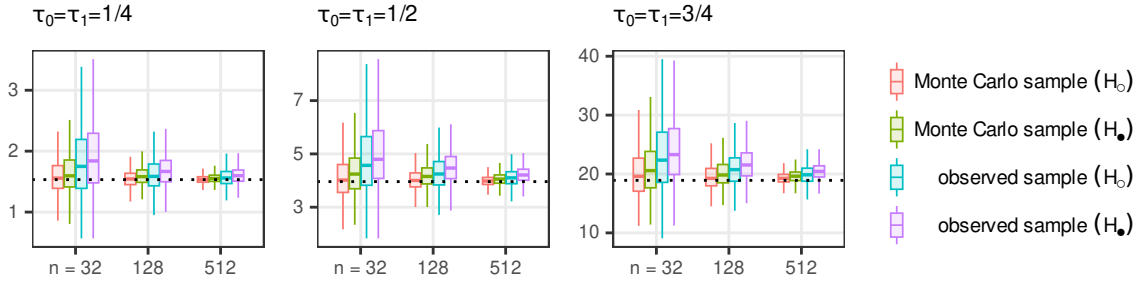


Figure 6: Boxplots comparing four estimators of Σ_{00} based on the methodology of §4 for a Clayton HAC with structure $\{\{1,2\},3\}$ and three pairs of identical parameters: $(\vartheta_0, \vartheta_1) = (\vartheta, \vartheta)$ with $\vartheta \in \{\theta : \tau_\psi(\theta) = 1/4, 1/2, 3/4\}$; the null hypothesis is $H_o : \vartheta_0 = \vartheta_1$. The four estimators are obtained by considering either $\hat{\theta}_o$ (H_o) or $\hat{\theta}_\bullet$ (H_\bullet), and either the observed sample (of size n) or a Monte Carlo sample (of size $N = 10^5$) generated from $C_{\hat{\theta}}$. The dashed lines indicate the true value of Σ_{00} , approximated using Monte Carlo sampling and the explicit formulas given in Appendix B.

gamma-clayton

5 Simulation study

c:sim-study

We now assess the finite sample performance of the tests described in §3, using the estimation methods for Σ described in §4 when necessary. To this end, we consider four types of hypotheses, described below, for which we generated datasets of sizes $n \in \{32, 128, 512\}$ using Gumbel, Clayton and Frank HACs involving two or three parameters. Recall the definition of τ_ψ^{-1} from §3.2. The parameters $(\vartheta_k)_{k=0}^K$, $K \in \{1, 2\}$ are chosen such that $\vartheta_k = \tau_\psi^{-1}(\tau_k) + \delta_k$ with $\tau_k \in \{1/4, 1/2, 3/4\}$ and $\delta_k \in \{0, 1/10\}$; non-zero δ_k values are used to create departures from the null. To further evaluate the impact of model misspecification, we model each dataset generated using Gumbel, Clayton and Frank HACs. For each scenario considered, empirical rejection rates given a nominal level of $\alpha = 0.05$ are computed from 1000 replications. The main conclusions are described below, while the full results are reported in Tables E.1–E.11 in Appendix E.¹

5.1 Scenario I: simple hypotheses

The first scenario treats the simple hypothesis $H_o : \vartheta_0 = \vartheta_1$ for a trivariate HAC with structure $\mathcal{G} = \{\{1,2\},3\}$ and parameters $\vartheta = (\vartheta_0, \vartheta_1)$, $\vartheta_0 \leq \vartheta_1$. Six combinations of parameters identified as Cases a–f are considered, of which only the first three are under the null. Tests were performed using both unconditional and conditional approaches; the mixture distribution of $W_1\chi_1^2$ given in Corollary 1 was used as the unconditional approach and χ_1^2 was used when $L_n > 0$ for the conditional approach as in Remark 3. The results are reported in Appendix Tables E.1–E.2.

We begin with the results for the unconditional test. When the null hypothesis is true and the fitted model coincides with that used to generate the data, the rejection rates agree with the nominal level, even for smaller sample sizes. However, when the fitted model does not coincide with

¹For estimators $\hat{\Sigma}$ of Σ based on Monte Carlo sampling, we use 10^5 replicates. When the distribution of L in Theorem 1 is not covered by one of the corollaries, we use 5×10^3 Monte Carlo replicates based on $Z \sim \mathcal{N}(\mathbf{h}, \hat{\Sigma})$ to approximate it.

that used to generate the data rejection rates are often dangerously larger than the nominal level. Surprisingly, this tendency reverses when the null hypothesis is false, as model misspecification leads to lower rejection rates in these cases. This highlights the importance of thoroughly assessing the fit of the chosen family prior to performing the test, and perhaps of selecting the best fitting family among a large variety of candidates. The results for Cases d–f also show that the test’s ability to identify departures from the null increases with the sample size and with the strength of the dependence, as expected.

The results for the conditional test follow a similar pattern than those of the unconditional test, the main difference being that the rejection rates are generally smaller. When the null is true and the model is correctly specified, the rejection rates are approximately half of those of the unconditional model, in accordance with Remark 3.

5.2 Scenario II: intersection hypotheses

In the second scenario, we consider the intersection hypothesis $H_o : \vartheta_0 = \vartheta_1 = \vartheta_2$ for four-variate HACs with structure $\mathcal{G} = \{\{1, 2\}, \{3, 4\}\}$. Nine combinations of parameters identified as Cases a–i are considered: $\vartheta_0 = \vartheta_1 = \vartheta_2$ for Cases a–c; $\vartheta_0 = \vartheta_1 < \vartheta_2$ for Cases d–f; and $\vartheta_0 < \vartheta_1 = \vartheta_2$ for Cases g–i. We test H_o using the unconditional test based on asymptotic null distribution of L_n given in Corollary 2 using the four different estimators of Σ appearing in Figure 6. All four estimators are obtained by inverting the observed Fisher information. They differ in the choice of estimate $\hat{\theta} \in \{\hat{\theta}_\bullet, \hat{\theta}_o\}$ at which the observed information is computed and the dataset used, either the observed sample or a Monte Carlo sample based on $\hat{\theta}$; see §4 for more details. The results are reported in Appendix Tables E.3–E.6.

The conclusions are broadly the same as for Scenario I. Unsurprisingly, the tests are more powerful against alternatives for which both $\vartheta_0 \neq \vartheta_1$ and $\vartheta_0 \neq \vartheta_2$, as in Cases g–i. More importantly, the results strongly suggest that the performance of the test is not robust to the choice of estimator $\hat{\Sigma}$. In particular, the estimators based on $\hat{\theta}_\bullet$ yields a liberal test under the null, while this is not the case for those based on $\hat{\theta}_o$.² In contrast, the estimation method for Σ had little impact on the performance of these tests. The superior performance of the estimator based on $\hat{\theta}_o$ is likely caused by the additional structure imposed on them; recall that some entries of Σ are equal under the null, and that the corresponding equalities are enforced in $\hat{\Sigma}$ when computed under H_o . This was also observed in a similar context in Perreault et al. (2023).

5.3 Scenario III: union hypotheses

In the third scenario, we generate the data as in Cases a–i of Scenario II, but we instead consider the union hypothesis $H_o : \vartheta_0 \in \{\vartheta_1, \vartheta_2\}$. To compute p -values, we use the one-component mixture consisting of χ_1^2 with probability 1/2 and zero otherwise, as suggested by Corollary 3. The results are reported in Appendix Table E.7.

Again, the results broadly agree the with those for Scenarios I and II. However, the rejection

²Note that some of the estimates $\hat{\Sigma}$ based on $\hat{\theta}_\bullet$ were not positive definite, making it impossible to compute p -values in these cases. This almost never occurred for cases when the null is satisfied, and occurred 164 times at of 1000 replications in the worst case. Replacing all the missing p -values by zero (or by one) has little effect on the results.

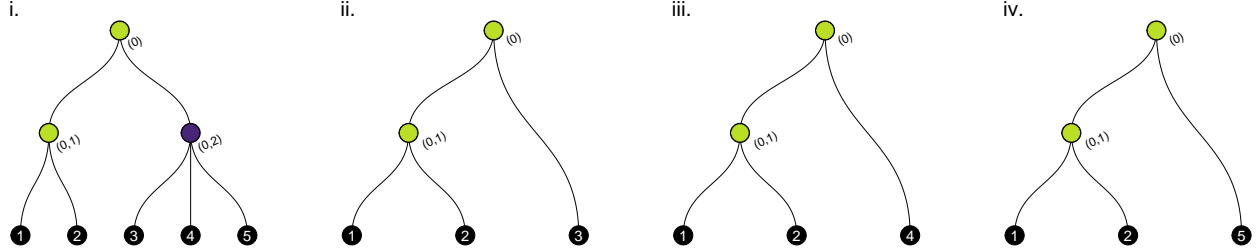


Figure 7: Simple example illustrating the construction of a HAC composite likelihood that is free of nuisance parameters. Consider a random vector (U_1, \dots, U_5) with a HAC distribution C_{ϑ} with corresponding tree structure as illustrated in Panel (i), where $\vartheta = (\vartheta_0, \vartheta_1, \vartheta_2)$ and ϑ_2 is a nuisance parameter. Panels (ii–iv) show the tree structures underlying the margins corresponding to (U_1, U_2, U_3) , (U_1, U_2, U_4) and (U_1, U_2, U_5) , respectively. Since none of them depend on ϑ_2 , they can be used to construct a composite likelihood free of ϑ_2 .

g:composite

rates are approximately equal to the nominal level only when either $\vartheta_0 = \vartheta_1$ or $\vartheta_0 = \vartheta_2$, but not both, which occurs only in Cases d–f. This highlights the fact by using the reference distribution described above we implicitly assume that at least one of ϑ_1 and ϑ_2 is different from ϑ_0 . Consequently, when this is not the case ($\vartheta_0 \notin \{\vartheta_1, \vartheta_2\}$), we obtain rejection rates that are conservative, and hence a lower than expected type I error at no cost in terms of type II error.

5.4 Scenario IV: simple hypotheses with nuisance

In the last scenario, we consider the simple hypothesis $H_o : \vartheta_0 = \vartheta_1$ of Scenario I, but this time with four-variate HACs as in Scenarios II and III. This introduces a nuisance parameter, which we deal with using the hybrid null distribution described in Remark 2. For comparison, we also test H_o assuming $\vartheta_0 = \vartheta_2$, in which case we follow Corollary 1 and compare L_n to the $(1 - 2\alpha)$ th quantile of a χ_1^2 . The results are reported in Appendix Tables E.8–E.11.

The results suggest that the hybrid method performs well in all six cases where the null is satisfied (Cases a–f). It thus compares favourably to the simplified method on that aspect, as the latter holds its level only when $\vartheta_0 = \vartheta_2$ (Cases a–c), and not when $\vartheta_0 \neq \vartheta_2$ (Cases d–f); this is more pronounced with large sample sizes n . Despite this, the empirical rejection rates associated with the hybrid method are only very slightly below those associated with the simplified method, whether or not $\vartheta_0 = \vartheta_2$.

6 Discussion

:discussion

In this paper, we studied asymptotic behavior of the maximum likelihood estimate and the likelihood ratio statistic testing for overparametrized HACs. As in Hofert et al. (2012), who studied likelihood inference for Archimedean copulas, we have assumed that the marginal distributions are known. Yet, we can draw conclusions that are likely to apply also in cases when the margins are estimated and when variants of maximum likelihood are used; e.g., two-stage (Genest et al., 1995; Joe, 1997), multistage (Okhrin et al., 2013), or multistage penalized (Okhrin and Ristig, 2024)

maximum likelihood.

Our theoretical results show that the asymptotic behavior of the maximum likelihood estimate and the likelihood ratio statistics can be very complex, depending on the geometry of the local parameter spaces under the null and alternative. In order to provide insight into how these quantities behave in practice we examined several shallow HACs with a single, one-parameter family of generators more carefully. As the asymptotic distribution of the likelihood ratio is not always available, we also discussed alternative approaches which condition on the region in which the maximum likelihood estimate lies; the drawback of this approach is that, without further modification, it is conservative. Some details on the approximation of the Fisher information matrix were provided, the discussion being specialized to cases where standard finite difference schemes cannot be used.

From Theorem 1, it is clear that when the generators are correctly specified and a reasonable initial (possibly overfitting) tree structure is set, maximum likelihood estimation has a positive probability of recovering the true tree structure. This has some implications on existing structure learning algorithms such as the one considered in Okhrin et al. (2013), where the collapse of a child node (\mathbf{i}, k) into its parent \mathbf{i} is triggered when $\hat{\theta}_{(\mathbf{i}, k)} - \hat{\theta}_{\mathbf{i}} < \epsilon$ for some small threshold parameter ϵ . From the same result it follows that the probability of recovering the true structure converges to one asymptotically. However, our results suggest that it might be beneficial to use distinct thresholds to collapse child-parent nodes, as the Fisher information matrix varies with the generator considered and the location of the true parameter. More generally they suggest that structure learning methods can benefit from using the information contained in the curvature of the log-likelihood as opposed to only relying on the difference between parameters; one such method, based on penalized estimation, was recently proposed by Okhrin and Ristig (2024).

Our work also raises some concerns about the practical usage of maximum likelihood inference and its variants. Our simulation study highlights that misspecifying the generators may lead to dramatically inflated rejection rates for structural likelihood ratio tests, which in turn suggests that structure learning algorithms are at risk of returning simplistic tree structures in most practical situations. A deeper analysis of our simulation results reveals that for a HAC with parameter ϑ in the interior of the parameter space, the best estimator given misspecified generators (e.g., $\boldsymbol{\eta}^*$ in Theorem 1 of Okhrin et al. (2013)) can lie on the boundary of the parameter space. This highlights the importance of considering a large family of generators, and further motivates the development of user-friendly estimation methods that allow mixing generator families within HACs. It also suggests that in cases when the object of inferential interest is the structure itself and not the parameters, nonparametric methods (Segers and Uyttendaele, 2014; Perreault et al., 2019; Zhang et al., 2021) might be more appropriate.

Finally, one of the main challenges underlying the implementation of the proposed tests is handling a large number of nuisance parameters. As a potential approach, we suggest investigating composite likelihood methods (Lindsay, 1988), which have been used by Cossette et al. (2019a), Chaoubi et al. (2021) and Górecki and Hofert (2023) in the context of HAC modeling. Specifically, one could construct an objective function by multiplying marginal likelihoods, as asymptotic guarantees are available for these constructions under some conditions; see, e.g., Varin (2008) and Varin et al. (2011). We illustrate this idea for a simple example in Figure 7, where one can elimi-

nate nuisance parameters at the cost of some loss in efficiency. Extending our results to composite likelihood inference under boundary conditions, following ideas in, e.g., Huang et al. (2020) and Azadbakhsh et al. (2021), could possibly provide likelihood ratio statistics whose distribution is free of nuisance parameters.

Acknowledgments

S.P. was supported by the Data Science Institute at the University of Toronto and N.R. was supported by the Natural Sciences and Engineering Research Council of Canada [grant number RGPIN-2020-05897].

References

- Cossette:2015 Abdallah, A., Boucher, J.-P., and Cossette, H. (2015). Modeling dependence between loss triangles with hierarchical Archimedean copulas. *ASTIN Bull.*, 45:577–599.
- Azadbakhsh/al:2021 Azadbakhsh, M., Gao, X., and Jankowski, H. (2021). Composite likelihood ratio testing under nonstandard conditions using tangent cones. *Stat*, 10:e375.
- Bartholomew:1959a Bartholomew, D. J. (1959a). A test of homogeneity for ordered alternatives. *Biometrika*, 46:36–48.
- Bartholomew:1959b Bartholomew, D. J. (1959b). A test of homogeneity for ordered alternatives. II. *Biometrika*, 46:328–335.
- Bartholomew:1961 Bartholomew, D. J. (1961). A test of homogeneity of means under restricted alternatives. *J. R. Stat. Soc. B*, 23:239–272.
- Chant:1974 Chant, D. (1974). On asymptotic tests of composite hypotheses in nonstandard conditions. *Biometrika*, 61:291–298.
- Chaoui/al:2021 Chaoubi, I., Cossette, H., Marceau, É., and Robert, C. Y. (2021). Hierarchical copulas with Archimedean blocks and asymmetric between-block pairs. *Comput. Stat. Data Anal.*, 154:107071.
- Chernoff:1954 Chernoff, H. (1954). On the distribution of the likelihood ratio. *Ann. Math. Stat.*, 25:573–578.
- Mtalai:2017 Cossette, H., Gadoury, S.-P., Marceau, É., and Mtalai, I. (2017). Hierarchical Archimedean copulas through multivariate compound distributions. *Insur. Math. Econ.*, 76:1–13.
- Robert:2019 Cossette, H., Gadoury, S.-P., Marceau, É., and Robert, C. Y. (2019a). Composite likelihood estimation method for hierarchical Archimedean copulas defined with multivariate compound distributions. *J. Multivar. Anal.*, 172:59–83. Dependence Models.
- Mtalai:2019 Cossette, H., Marceau, É., and Mtalai, I. (2019b). Collective risk models with dependence. *Insur. Math. Econ.*, 87:153–168.
- Rivest:1995 Genest, C., Ghouli, K., and Rivest, L.-P. (1995). A semiparametric estimation procedure of dependence parameters in multivariate families of distributions. *Biometrika*, 82:543–552.
- Rivest:1993 Genest, C. and Rivest, L.-P. (1993). Statistical inference procedures for bivariate Archimedean copulas. *J. Am. Stat. Assoc.*, 88:1034–1043.

- Geyer:1994 Geyer, C. J. (1994). On the asymptotics of constrained M -estimation. *Ann. Stat.*, 22:1993–2010.
- Haynsworth:1972 Goldberg, K., Newman, M., and Haynsworth, E. V. (1972). Combinatorial analysis. In Abramowitz, M. and Stegun, I. A., editors, *Handbook of Mathematical Functions*, chapter 24. National Bureau of Standards. Applied Mathematics Series 55. Tenth Printing.
- Hofert:2015 Grothe, O. and Hofert, M. (2015). Construction and sampling of Archimedean and nested Archimedean Lévy copulas. *J. Multivar. Anal.*, 138:182–198.
- Hofert:2023 Górecki, J. and Hofert, M. (2023). Composite pseudo-likelihood estimation for pair-tractable copulas such as Archimedean, Archimax and related hierarchical extensions. *J. Stat. Comput. Simul.*, 93:2321–2355.
- Holeňa:2017-DM Górecki, J., Hofert, M., and Holeňa, M. (2017a). Kendall’s tau and agglomerative clustering for structure determination of hierarchical Archimedean copulas. *Dependence Modeling*, 5:75–87.
- Holeňa:2017-JSCS Górecki, J., Hofert, M., and Holeňa, M. (2017b). On structure, family and parameter estimation of hierarchical Archimedean copulas. *J. Stat. Comput. Simul.*, 87:3261–3324.
- Okhrin:2021 Górecki, J., Hofert, M., and Okhrin, O. (2021). Outer power transformations of hierarchical Archimedean copulas: Construction, sampling and estimation. *Comput. Stat. Data Anal.*, 155:107109.
- Hering/al:2010 Hering, C., Hofert, M., Mai, J.-F., and Scherer, M. (2010). Constructing hierarchical Archimedean copulas with Lévy subordinators. *J. Multivar. Anal.*, 101:1428–1433.
- Hofert:2010 Hofert, M. (2010). *Sampling nested Archimedean copulas with applications to CDO pricing*. PhD thesis, Universität Ulm.
- Hofert:2011 Hofert, M. (2011). Efficiently sampling nested Archimedean copulas. *Comput. Stat. Data Anal.*, 55:57–70.
- copula:2023 Hofert, M., Kojadinovic, I., Maechler, M., and Yan, J. (2023). *copula: Multivariate Dependence with Copulas*. R package version 1.1-2.
- Mächler:2011 Hofert, M. and Mächler, M. (2011). Nested Archimedean copulas meet R: The nacopula package. *J. Stat. Software*, 39:1–20.
- McNeil:2012 Hofert, M., Mächler, M., and McNeil, A. J. (2012). Likelihood inference for Archimedean copulas in high dimensions under known margins. *J. Multivar. Anal.*, 110:133–150.
- Hofert/Pham:2013 Hofert, M. and Pham, D. (2013). Densities of nested Archimedean copulas. *J. Multivar. Anal.*, 118:37–52.
- Scherer:2011 Hofert, M. and Scherer, M. (2011). CDO pricing with nested Archimedean copulas. *Quant. Finance*, 11:775–787.
- Ščavnický:2015 Holeňa, M., Bajer, L., and Ščavnický, M. (2015). Using copulas in data mining based on the observational calculus. *IEEE Trans. Knowl. Data Eng.*, 27:2851–2864.
- Cai/al:2020 Huang, J., Ning, Y., Cai, Y., Liang, K.-Y., and Chen, Y. (2020). Composite likelihood inference under boundary conditions. *Stat. Sin.*, 30:1005–1025.
- Joe:1997 Joe, H. (1997). *Multivariate models and multivariate dependence concepts*. CRC press.

- Kudo:1963 Kudo, A. (1963). A multivariate analogue of the one-sided test. *Biometrika*, 50:403–418.
- Li/Liu:2021 Li, J., Balasooriya, U., and Liu, J. (2021). Using hierarchical Archimedean copulas for modelling mortality dependence and pricing mortality-linked securities. *Ann. Actuar. Sci.*, 15:505–518.
- Lindsay:1988 Lindsay, B. G. (1988). Composite likelihood methods. *Comtemp. Math.*, 80:221–239.
- Matsypura/et al:2016 Matsypura, D., Neo, E., and Prokhorov, A. (2016). Estimation of hierarchical Archimedean copulas as a shortest path problem. *Econ. Lett.*, 149:131–134.
- McNeil:2008 McNeil, A. J. (2008). Sampling nested Archimedean copulas. *J. Stat. Comput. Simul.*, 78:567–581.
- McNeil/Nešlehová:2009 McNeil, A. J. and Nešlehová, J. (2009). Multivariate Archimedean copulas, d-monotone functions and ℓ_1 -norm symmetric distributions. *Ann. Stat.*, 37:3059–3097.
- Moran:1971b Moran, P. A. P. (1971). Maximum-likelihood estimation in non-standard conditions. *Math. Proc. Cambridge Philos. Soc.*, 70:441–450.
- Nelsen/et al:2003 Nelsen, R. B., Quesada-Molina, J. J., Rodríguez-Lallena, J. A., and Úbeda Flores, M. (2003). Kendall distribution functions. *Stat. Probab. Lett.*, 65:263–268.
- Okhrin/Schmid:2013 Okhrin, O., Okhrin, Y., and Schmid, W. (2013). On the structure and estimation of hierarchical Archimedean copulas. *J. Econom.*, 173:189–204.
- Okhrin/Ristig:2014 Okhrin, O. and Ristig, A. (2014). Hierarchical Archimedean Copulae: The HAC Package. *J. Stat. Software*, 58:1–20.
- Okhrin/Ristig:2024 Okhrin, O. and Ristig, A. (2024). Penalized estimation of hierarchical Archimedean copula. *J. Multivar. Anal.*, 201:105274.
- Perreault:2020 Perreault, S. (2020). *Structures de corrélation partiellement échangeables*. PhD thesis, Université Laval.
- Perreault/Duchesne/Nešlehová:2019 Perreault, S., Duchesne, T., and Nešlehová, J. G. (2019). Detection of block-exchangeable structure in large-scale correlation matrices. *J. Multivar. Anal.*, 169:400–422.
- Perreault/Duchesne/Nešlehová:2023 Perreault, S., Nešlehová, J. G., and Duchesne, T. (2023). Hypothesis tests for structured rank correlation matrices. *J. Am. Stat. Assoc.*, 118:2889–2900.
- Rezapour:2015 Rezapour, M. (2015). On the construction of nested Archimedean copulas for d-monotone generators. *Stat. Probab. Lett.*, 101:21–32.
- Savu/Trede:2010 Savu, C. and Trede, M. (2010). Hierarchies of Archimedean copulas. *Quant. Finance*, 10:295–304.
- Segers/Uyttendaele:2014 Segers, J. and Uyttendaele, N. (2014). Nonparametric estimation of the tree structure of a nested Archimedean copula. *Comput. Stat. Data Anal.*, 72:190–204.
- Self/Liang:1987 Self, S. G. and Liang, K.-Y. (1987). Asymptotic properties of maximum likelihood estimators and likelihood ratio tests under nonstandard conditions. *J. Am. Stat. Assoc.*, 82:605–610.
- Shapiro:1985 Shapiro, A. (1985). Asymptotic distribution of test statistics in the analysis of moment structures under inequality constraints. *Biometrika*, 72:133–144.
- Shapiro:2000 Shapiro, A. (2000). On the asymptotics of constrained local M -estimators. *Ann. Stat.*, 28:948–960.

- Susko:2013 Susko, E. (2013). Likelihood ratio tests with boundary constraints using data-dependent degrees of freedom. *Biometrika*, 100:1019–1023.
- Uyttendaele:2018 Uyttendaele, N. (2018). On the estimation of nested Archimedean copulas: a theoretical and an experimental comparison. *Comput. Stat.*, 33:1047–1070.
- van der Vaart:1998 van der Vaart, A. W. (1998). *Asymptotic Statistics*. Cambridge University Press.
- Varin:2008 Varin, C. (2008). On composite marginal likelihoods. *AStA Adv. Stat. Anal.*, 92:1–28.
- Varin/Firth:2011 Varin, C., Reid, N., and Firth, D. (2011). An overview of composite likelihood methods. *Statistica Sinica*, 21:5–42.
- Whelan:2004 Whelan, N. (2004). Sampling from Archimedean copulas. *Quant. Finance*, 4:339–352.
- Zhang/Jin/Bai:2021 Zhang, W., Jin, B., and Bai, Z. (2021). Learning block structures in U-statistic-based matrices. *Biometrika*, 108(4):933–946.
- Zhu/Tan:2016 Zhu, W., Wang, C.-W., and Tan, K. S. (2016). Structure and estimation of Lévy subordinated hierarchical Archimedean copulas (LSHAC): Theory and empirical tests. *J. Banking Finance*, 69:20–36.

A Proofs

app:proofs

Proof of Corollary 1

In this case, $\mathcal{A} = \{\mathbf{z} : z_1 \leq z_2\}$ is a half space whose only boundary is $\mathcal{A}_o = \{\mathbf{z} : z_1 = z_2\}$. The Gaussian vector $\mathbf{Z} = (Z_0, Z_1)$ in Theorem 1, centered at $(0, 0) \in \mathcal{A}_o$, is thus equally likely to fall on either side \mathcal{A}_o , regardless of Σ . When $Z_0 \geq Z_1$, then \mathbf{Z}_\bullet lies on \mathcal{A}_o , implying $\mathbf{Z}_o = \mathbf{Z}_\bullet$ and therefore $L_n = L_\infty = 0$ with probability one. In the other case when $Z_0 < Z_1$, then $\mathbf{Z}_\bullet = \mathbf{Z}$ and $\mathbf{Z}_o = \mathbf{P}_o \mathbf{Z}$, for some matrix \mathbf{P}_o of rank 2. One can check that Lemma 1 holds with $\mathbf{P} = \mathbf{I} - \mathbf{P}_o$, which implies $(L_\infty | \mathbf{Z} \in \mathcal{A}) \sim \chi_1^2$, from which the result follows.

Additional notation for the proofs of Corollaries 2, 3 and 5, below. Instead of \mathbf{Z} , we consider $\mathbf{Z}^* := (Z_1, Z_2) - Z_0$, whose distribution is given by $\mathbf{Z}^* \sim \mathcal{N}(\mathbf{0}, \Sigma_*)$, where $\Sigma_* = \sigma_0^2 - 2\sigma_{01} + \sigma_1^2 \mathbf{I} + (1 - \mathbf{I})\sigma_{12}$. Denote the two-dimensional analogues of \mathcal{A} and \mathcal{A}_o associated with \mathbf{Z}^* by \mathcal{A}^* and \mathcal{A}_o^* (see Figure A.1 for depictions of \mathcal{A}^* in specific cases), and the projection of \mathbf{Z}^* onto \mathcal{A}^* and \mathcal{A}_o^* by \mathbf{Z}_\bullet^* and \mathbf{Z}_o^* , respectively. Also define $\beta := (\sigma_0^2 - 2\sigma_{01} + \sigma_{12}) / (\sigma_0^2 - 2\sigma_{01} + \sigma_1^2)$.

Proof of Corollary 2

One can verify that $L_\infty = q\mathbf{z}^*(\mathbf{Z}_o^*) - q\mathbf{z}^*(\mathbf{Z}_\bullet^*)$ and that Σ_* has eigenvalues $\lambda_\pm = (1 \pm 1)(\sigma_0^2 - 2\sigma_{01}) + \sigma_1^2 \pm \sigma_{12}$ with corresponding eigenvectors $\mathbf{v}_\pm = (1, \pm 1)/\sqrt{2}$. Also note that $\mathcal{A}^* = \{\mathbf{z} : z \geq \mathbf{0}\}$ and $\mathcal{A}_o^* = \{(0, 0)\}$ in this case, and let \mathcal{L}_y and \mathcal{L}_x be the vertical and horizontal boundaries of \mathcal{A}^* .

In what follows, we partition \mathbb{R}^2 into four disjoint (up to zero-probability sets) cones based on the matrix $\mathbf{P} = \mathbf{P}_\bullet - \mathbf{P}_o$ as given in Lemma 1. Specifically, we write $\mathbb{R}^2 = \mathcal{C}_0 \cup \mathcal{C}_1^x \cup \mathcal{C}_1^y \cup \mathcal{C}_2$, with $\mathcal{C}_0 := \mathbf{P}_\bullet^{-1} \mathcal{A}_o^*$, $\mathcal{C}_1^x := \mathbf{P}_\bullet^{-1} \mathcal{L}_x$, $\mathcal{C}_1^y := \mathbf{P}_\bullet^{-1} \mathcal{L}_y$, and $\mathcal{C}_2 := \mathbf{P}_\bullet^{-1} \mathbb{R}_+^2$, respectively, where \mathbf{P}_\bullet and \mathbf{P}_o are the operators projecting $\mathbf{z} \in \mathbb{R}^2$ onto \mathcal{A}^* and \mathcal{A}_o^* based on the Mahalanobis distance characterized by Σ_*^{-1} . Further let $\mathcal{C}_1 := \mathcal{C}_1^y \cup \mathcal{C}_1^x$. One can verify using Lemma 1 that $(L_\infty | \mathbf{Z}^* \in \mathcal{C}_k) \sim \chi_k^2$ for $k = 0, 1, 2$; it remains to determine $\gamma_k := \mathbb{P}(\mathbf{Z}^* \in \mathcal{C}_k)$ for each k .

Following (Shapiro, 1985, p. 140), we compute γ_0 by finding the opening angle α_0 of the cone $\Sigma_*^{-1/2} \mathcal{C}_0$, whose upper and lower boundaries are the half lines $\mathcal{L}_\pm := \{\mathbf{z} : z_1 = a(\lambda_+ \pm \lambda_-), z_2 = a(\lambda_+ \mp \lambda_-), a \in \mathbb{R}_-\}$, respectively. More precisely, we have $\gamma_0 = \alpha_0 / (2\pi)$, where $\alpha_0 = \cos^{-1}(\mathbf{w}_+^\top \mathbf{w}_-)$ with $\mathbf{w}_\pm \in \Sigma_*^{-1/2} \mathcal{L}_\pm$ such that $\|\mathbf{w}_\pm\| = 1$. Through algebraic manipulations we can show that $\mathbf{w}_\pm = (\sqrt{\lambda_+} \mathbf{v}_+ \pm \sqrt{\lambda_-} \mathbf{v}_-) / \sqrt{\lambda_+ + \lambda_-}$, and thus $\mathbf{w}_+^\top \mathbf{w}_- = (\lambda_+ - \lambda_-) / (\lambda_+ + \lambda_-) = (\sigma_0^2 - 2\sigma_{01} + \sigma_{12}) / (\sigma_0^2 - 2\sigma_{01} + \sigma_1^2) = \beta$.

To compute γ_1 , first note that $\mathbb{P}(\mathbf{Z}^* \in \mathcal{C}_1^y) = \mathbb{P}(\mathbf{Z}^* \in \mathcal{C}_1^x)$, and so $\gamma_1 = 2\mathbb{P}(\mathbf{Z}^* \in \mathcal{C}_1^y)$. Also, \mathcal{C}_1^y has boundaries given by \mathcal{L}_+ and \mathcal{L}_y . For any vector $\mathbf{z}_+ \in \mathcal{L}_+$, we have $\mathbf{z}_+^\top \Sigma_*^{-1} \in \mathcal{L}_x$, and hence $\mathbf{z}_+^\top \Sigma_*^{-1} \mathbf{z} = 0$ for any $\mathbf{z} \in \mathcal{L}_y$. The opening angle can thus be obtained as $\alpha_1^+ = \cos^{-1}(0) = \pi/2$, and so $\gamma_1 = 2\mathbb{P}(\mathbf{Z}^* \in \mathcal{C}_1^y) = 2\alpha_1^+ / (2\pi) = 1/2$ and $\gamma_2 = 1 - \gamma_1 - \gamma_0 = 1/2 - \gamma_0$.

Proof of Corollary 3

For the case when $\vartheta_0 = \vartheta_1 < \vartheta_2$, we have that \mathcal{A}^* is the right half-plane $(\{0\} \cup \mathbb{R}_+) \times \mathbb{R}$ and \mathcal{A}_o^* the vertical line $\{0\} \times \mathbb{R}$. The result follows from the proof of Corollary 1.

For the case, $\vartheta_0 = \vartheta_1 = \vartheta_2$, recall the definitions of \mathcal{L}_x , \mathcal{L}_y , \mathcal{L}_- and \mathcal{L}_+ from the proof of Corollary 2, and note that $\mathcal{A}^* = (\mathbb{R}_+ \cup \{0\})^2$ and $\mathcal{A}_o^* = \{(0, 0)\} \cup \mathcal{L}_y \cup \mathcal{L}_x$. Further denote by \mathbf{Z}^x and \mathbf{Z}^y the projections of \mathbf{Z}^* onto \mathcal{L}_x and \mathcal{L}_y , respectively. We consider the two cases $\beta > 0$ and $\beta \leq 0$ separately.

For the case $\beta > 0$, consider the sets \mathcal{C}_0 , \mathcal{C}_1^x , \mathcal{C}_1^y and \mathcal{C}_2 , as defined in the proof of Corollary 2

(i.e., as in Figure A.2.i), and we partition $\mathcal{C}_2 = \mathbb{R}_+^2$ in three regions in a similar fashion such that \mathcal{C}_0 , $(\mathcal{C}_1^x \cap \mathbb{R}_-^2)$ and $(\mathcal{C}_1^y \cap \mathbb{R}_-^2)$ partition \mathbb{R}_-^2 . Denote the resulting cones \mathcal{C}_2^x (with boundaries $-\mathcal{L}_+$ and \mathcal{L}_x), \mathcal{C}_2^y (with boundaries $-\mathcal{L}_-$ and \mathcal{L}_y) and \mathcal{C}_2^0 (with boundaries $-\mathcal{L}_+$ and $-\mathcal{L}_-$) and note that $L_\infty = \min\{q_{\mathbf{Z}}(\mathbf{Z}^x), q_{\mathbf{Z}}(\mathbf{Z}^y)\}$, which always equals $q_{\mathbf{Z}}(\mathbf{Z}^x)$ when $\mathbf{Z}^* \in \mathcal{C}_2^x$ and $q_{\mathbf{Z}}(\mathbf{Z}^y)$ when $\mathbf{Z}^* \in \mathcal{C}_2^y$. Further note that $\mathbb{P}(\mathbf{Z}^* \in \mathcal{C}_2^0) = \gamma_0$, and thus

$$\mathbb{P}(\mathbf{Z}^* \in \mathcal{D}^x) = \mathbb{P}(\mathbf{Z}^* \in \mathcal{D}^y) = (\gamma_2 - \gamma_0)/2 + \gamma_0 = 1/4 \quad \mathcal{D}^x := \mathcal{C}_2^x \cup \mathcal{C}_2^0, \quad \mathcal{D}^y := \mathcal{C}_2^y \cup \mathcal{C}_2^0,$$

and by Lemma 1, $(q_{\mathbf{Z}}(\mathbf{Z}^x)|\mathbf{Z}^* \in \mathcal{D}^x) \sim \chi_1^2$ and $(q_{\mathbf{Z}}(\mathbf{Z}^y)|\mathbf{Z}^* \in \mathcal{D}^y) \sim \chi_1^2$. Combining all this, we get

$$\begin{aligned} \mathbb{P}(L_\infty > z) &= \mathbb{P}(L_\infty > z \cap \mathbf{Z}^* \in \mathcal{C}_2) = \mathbb{P}\{(L_\infty > z \cap \mathbf{Z}^* \in \mathcal{D}^x) \cup (L_\infty > z \cap \mathbf{Z}^* \in \mathcal{D}^y)\} \\ &\leq \mathbb{P}(L_\infty > z \cap \mathbf{Z}^* \in \mathcal{D}^x) + \mathbb{P}(L_\infty > z \cap \mathbf{Z}^* \in \mathcal{D}^y) = 2\mathbb{P}(L_\infty > z \cap \mathbf{Z}^* \in \mathcal{D}^x) \\ &= 2\mathbb{P}(\mathbf{Z}^* \in \mathcal{D}^x) \mathbb{P}(L_\infty > z | \mathbf{Z}^* \in \mathcal{D}^x) < (1/2)\mathbb{P}\{\chi_1^2 > z\}, \end{aligned}$$

since $L_\infty = \min\{q_{\mathbf{Z}}(\mathbf{Z}^x), q_{\mathbf{Z}}(\mathbf{Z}^y)\} \leq q_{\mathbf{Z}}(\mathbf{Z}^x)$ when $\mathbf{Z}^* \in \mathcal{D}^x$. In other words, $L_\infty \preceq W\xi$ for $W \sim \mathcal{B}(1/2)$ and some ξ such that $\mathbb{P}(\xi > x) < \mathbb{P}(\chi_1^2 > x)$.

When $\beta \leq 0$, the cones \mathcal{C}_2^x (with boundaries $-\mathcal{L}_+$ and \mathcal{L}_x) and \mathcal{C}_2^y (with boundaries $-\mathcal{L}_-$ and \mathcal{L}_y) are no longer contained in $\mathcal{C}_2 = \mathbb{R}_+^2$. In fact, $\mathcal{C}_2^x \subset \mathcal{C}_1^x \subseteq \mathbb{R}_+ \times \mathbb{R}_-$ and $\mathcal{C}_2^y \subset \mathcal{C}_1^y \subseteq \mathbb{R}_- \times \mathbb{R}_+$; see Figure A.2.ii. By design we still have that $(q_{\mathbf{Z}}(\mathbf{Z}^x)|\mathbf{Z}^* \in \mathcal{C}_2 \cup \mathcal{E}^x) \sim \chi_1^2$, $(q_{\mathbf{Z}}(\mathbf{Z}^y)|\mathbf{Z}^* \in \mathcal{C}_2 \cup \mathcal{E}^y) \sim \chi_1^2$, and

$$\mathbb{P}(\mathbf{Z}^* \in \mathcal{D}^x) = \mathbb{P}(\mathbf{Z}^* \in \mathcal{D}^y) = \mathbb{P}(\mathbf{Z}^* \in \mathcal{C}_2^x) + \mathbb{P}(\mathbf{Z}^* \in \mathcal{C}_2) = (\gamma_0 - \gamma_2)/2 + \gamma_2 = 1/4.$$

Hence,

$$\begin{aligned} \mathbb{P}(L_\infty > z) &= \mathbb{P}\{L_\infty > z \cap (\mathbf{Z}^* \in \mathcal{E}^x \cup \mathcal{C}_2 \cup \mathcal{E}^y)\} \\ &= \mathbb{P}\{(L_\infty > z \cap \mathbf{Z}^* \in \mathcal{D}^x) \cup (L_\infty > z \cap \mathbf{Z}^* \in \mathcal{D}^y)\} \\ &\leq \mathbb{P}(L_\infty > z \cap \mathbf{Z}^* \in \mathcal{D}^x) + \mathbb{P}(L_\infty > z \cap \mathbf{Z}^* \in \mathcal{D}^y) \\ &= 2\mathbb{P}(L_\infty > z \cap \mathbf{Z}^* \in \mathcal{D}^x) \\ &= 2\mathbb{P}(\mathbf{Z}^* \in \mathcal{D}^x) \mathbb{P}(L_\infty > z | \mathbf{Z}^* \in \mathcal{D}^x) \\ &< (1/2)\mathbb{P}\{\chi_1^2 > z\}, \end{aligned}$$

since

$$(L_\infty | \mathbf{Z}^* \in \mathcal{D}^x) = (\mathbb{1}\{\mathbf{Z}^* \in \mathcal{C}_2\} \min\{q_{\mathbf{Z}}(\mathbf{Z}^x), q_{\mathbf{Z}}(\mathbf{Z}^y)\} | \mathbf{Z}^* \in \mathcal{D}^x) \leq (q_{\mathbf{Z}}(\mathbf{Z}^x) | \mathbf{Z}^* \in \mathcal{D}^x).$$

This concludes the proof.

Proof of Corollary 5

Use the notation of Corollary 2, but this time define the null space as $\mathcal{A}_\circ^* = \{(0, 0)\} \cup \mathcal{L}_y$. Now, if $\mathbf{Z}^* \in \mathcal{C}_0 \cup \mathcal{C}_1^y$ then $\mathbf{Z}_\bullet^* \in \mathcal{A}_\circ^*$, and so $L_\infty = 0$ with probability one. If $\mathbf{Z}^* \in \mathcal{C}_1^x$, then $\mathbf{Z}_\bullet^* \in \mathcal{L}_1^-$ and $\mathbf{Z}_\circ^* = (0, 0)$; an application of Lemma 1 shows that $(L_\infty | \mathbf{Z}^* \in \mathcal{C}_1^x) \sim \chi_1^2$.

To treat the case $\mathbf{Z}^* \in \mathcal{C}_2$, consider the partition $\mathcal{C}_2 = \mathcal{C}_2^x \cup \mathcal{C}_2^0 \cup \mathcal{C}_2^y$ as defined in the proof of Corollary 3. When $\mathbf{Z}^* \in \mathcal{C}_2^x \cup \mathcal{C}_2^0$, then $\mathbf{Z}_\bullet^* = \mathbf{Z}^*$ and $\mathbf{Z}_\circ^* \in \mathcal{L}_y$, meaning that $(L_\infty | \mathbf{Z}^* \in \mathcal{C}_2^x \cup \mathcal{C}_2^0) \sim \chi_1^2$. In contrast, if $\mathbf{Z}^* \in \mathcal{C}_2^y$ then $\mathbf{Z}_\bullet^* = \mathbf{Z}^*$ and $\mathbf{Z}_\circ^* = (0, 0)$, and so $(L_\infty | \mathbf{Z}^* \in \mathcal{C}_2^y) \sim \chi_2^2$. Note that,

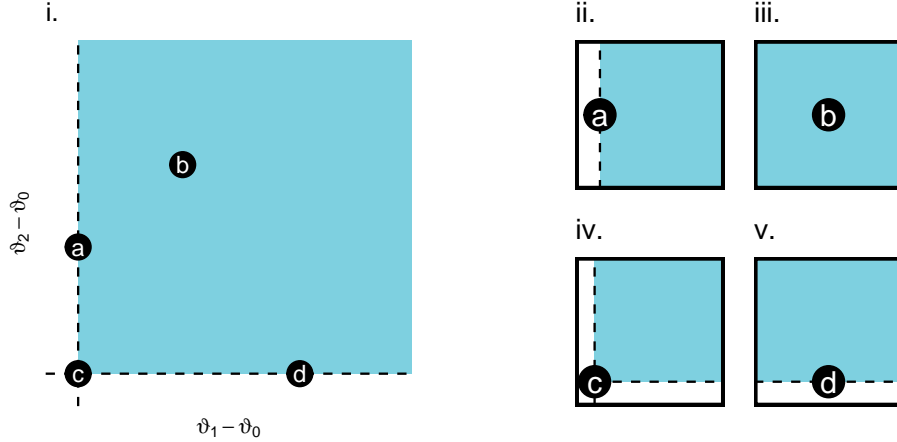


Figure A.1: (i) Depiction, in the two-dimensional plane, of the three-dimensional parameter space Θ for a two-level HAC with parameters ϑ_0 , ϑ_1 and ϑ_2 . (ii–v) Depiction of the asymptotic local parameter space \mathcal{A}^* associated with \mathbf{Z}^* as defined in the proofs of Corollaries 2, 3, and 5. More specifically, (ii) arises when $\vartheta_0 = \vartheta_1 < \vartheta_2$; (iii) arises when $\vartheta_0 < \vartheta_1, \vartheta_2$; (iv) arises when $\vartheta_0 = \vartheta_1 = \vartheta_2$; and (v) arises when $\vartheta_0 = \vartheta_2 < \vartheta_1$.

Complement to Remark 2: Consider testing $H_o : \vartheta_0 = \vartheta_1$ against $H_\bullet : \vartheta_0 < \vartheta_1$ in the presence of a nuisance parameter ϑ_2 with the hybrid null distribution discussed in Remark 2. The null distribution in question is that of normal random vector $\mathbf{Z}_n = (Z_{0n}, Z_{1n}, Z_{2n})$ centered at $\sqrt{n}(0, 0, h_n)$, where $h_n = \hat{\theta}_2 - \hat{\theta}_0$. To get some intuition, one may instead focus on $\mathbf{Z}_n^* = (Z_{1n}^*, Z_{2n}^*) = (Z_{1n} - Z_{0n}, Z_{2n} - Z_{0n})$, whose distribution is normal and centered at $(0, h_n)$. Regardless of the value of $\vartheta_2 - \vartheta_0$, the local parameter space \mathcal{A}^* associated with \mathbf{Z}_n^* is that given in panel (iv), and the associated local null space \mathcal{A}_o^* is the non-negative y-axis defined by $Z_{2n}^* = 0$, that is, $Z_{0n} = Z_{2n}$. However, when $\vartheta_0 < \vartheta_2$, then $h_n \rightarrow \infty$ as $n \rightarrow \infty$ and the probability that $Z_{1n}^* = 0$ vanishes. Therefore, it does not make a difference to assume that \mathcal{A}^* is as in panel (ii), which leads to a null distribution for \mathbf{Z} as in the setup of Corollary 3 ($\vartheta_0 = \vartheta_1 < \vartheta_2$) and Corollary 4. If instead $\vartheta_0 = \vartheta_2$, then h_n does not converge to zero as $n \rightarrow \infty$. In this case the distribution of \mathbf{Z}_n^* is centered somewhere on the non-negative part of the y-axis (possibly at $(0, 0)$, but not necessarily), but the probability that $Z_{2n} = 0$ does not vanish as $n \rightarrow \infty$ and \mathcal{A}^* may not coincide with (ii).

fig:sets2

although it is not shown here, the application of Lemma 1 used to derive the last two conditional distributions is valid only when $\beta \geq 0$, hence the additional condition in this corollary's statement.

By the same reasoning as in the proof of Corollary 3, we get $\gamma := \mathbb{P}(\mathbf{Z}^* \in \mathcal{C}_2^y) = \gamma_0 + (\gamma_2 - \gamma_0)/2 = 1/4 - \cos^{-1}(\beta)$, and hence $\gamma_1'' = \mathbb{P}(\mathbf{Z}^* \in \mathcal{C}_1^x) + \mathbb{P}(\mathbf{Z}^* \in \mathcal{C}_2) - \mathbb{P}(\mathbf{Z}^* \in \mathcal{C}_2^y) = \gamma_1 + \gamma_2 - \gamma = 1/2$ and $\gamma_2'' = \mathbb{P}(\mathbf{Z}^* \in \mathcal{C}_2^y) = \gamma$.

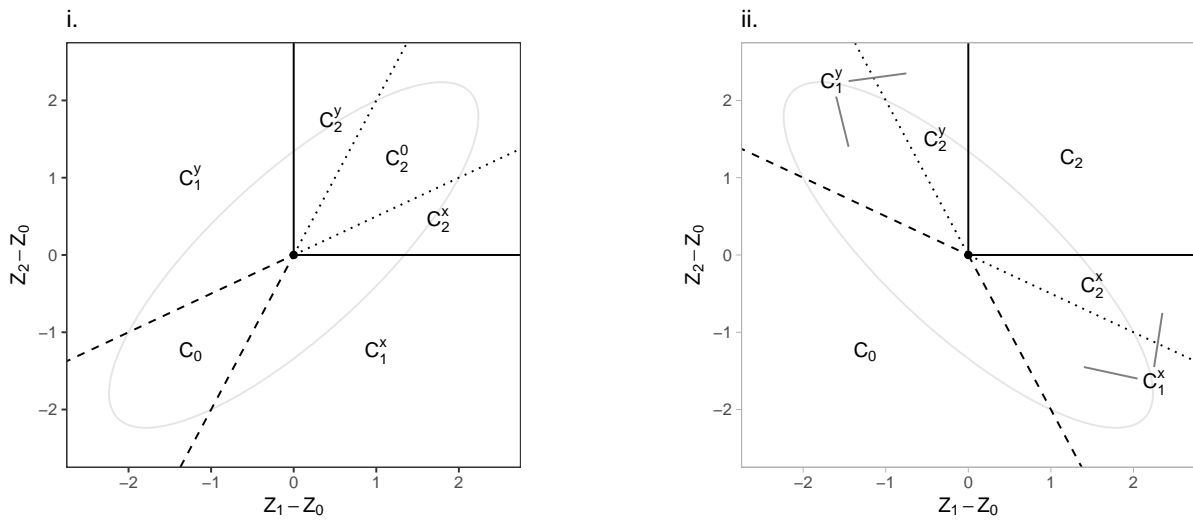


Figure A.2: Partition of \mathbb{R}^2 used in the proofs of Corollaries 2, 3 and 5. They are characterized by the half-lines $\mathcal{L}_x := \mathbb{R}_+ \times \{0\}$ and $\mathcal{L}_y := \{0\} \times \mathbb{R}_+$, the dashed half-lines \mathcal{L}_- and \mathcal{L}_+ and their reflections, the dotted half-lines $-\mathcal{L}_-$ and $-\mathcal{L}_+$; \mathcal{L}_- and $-\mathcal{L}_-$ are the ones with steepest slopes. Panel (i) depicts the case $\beta > 0$, for which $C_2 = C_2^x \cup C_2^0 \cup C_2^y$. Panel (ii) depicts the case $\beta < 0$, for which $C_2^x \subset C_1^x$ and $C_2^y \subset C_1^y$. For reference, a level set of the Gaussian density with covariance $\text{Cov}(Z_1 - Z_0, Z_2 - Z_0)$ is shown in gray.

fig:proofs

B Two-level HACs

In this section, we consider two-level HACs generated by a single one parameter family with ∞ -monotone generators. Specifically, we provide analytic formulas for the first- and second-order derivatives of commonly used families of copulas and explicit formulas for the Clayton and Gumbel generators. We begin with some notation and formulas for HAC densities specific for two level HACs.

B.1 Restricted framework, general notation and HAC density

To ease the notation, we let $K := K_0$ and drop the vector-index notation by using k instead of $(0, k)$ to index the elements associated with node $(0, k)$, for example $\psi_k := \psi_{(0,k)}$ and let $\mathcal{I} := \{0, \dots, K\}$. Also recall that $d := \sum_{i=1}^K d_i$ and let $\mathbf{d} := (d_i)_{i=1}^K$. Additionally, we follow Hofert and Pham (2013) and define

$$t_i(\mathbf{u}_i) := \sum_{j=1}^{d_i} \phi_i(u_{ij}), \quad \mathbf{t}(\mathbf{u}) := \{t_i(\mathbf{u}_i)\}_{i=1}^K \quad \text{and} \quad t(\mathbf{u}) := \sum_{i=1}^K \phi_0(C_i(\mathbf{u}_i)),$$

for $i = 1, \dots, K$, $\mathbf{u}_i = (u_{ij})_{j=1}^{d_i} \in (0, 1)^{d_i}$ and $\mathbf{u} = (\mathbf{u}_i)_{i=1}^K$. Note that t_i and t are such that $C_i = \psi_i \circ t_i$ and $C = \psi_0 \circ t$.

In what follows, as well as in Tables B.1–B.6, we use the *prime* symbol to denote the first-order derivative of a function with respect to its argument, and parenthesized integers to denote higher-order derivatives. When a function involves only one parameter, we use the dot and double dot symbols to denote its first- and second-order partial derivatives with respect to the parameter. If the function involves multiple parameters, then we replace the dots by the indices of the parameters with respect to which the derivatives are taken (see, e.g., Table B.5), which allows more compact formulas. For example, we define the derivatives of the generator ψ_θ as

$$\begin{aligned} \psi'_\theta(t) &:= \frac{\partial}{\partial t} \psi_\theta(t), & \psi_\theta^{(k)}(t) &:= \frac{\partial^k}{\partial t^k} \psi_\theta(t), & \dot{\psi}_\theta(t) &:= \frac{\partial}{\partial \theta} \psi_\theta(t), \\ \ddot{\psi}_\theta(t) &:= \frac{\partial^2}{\partial \theta^2} \psi_\theta(t), & \dot{\psi}'_\theta(t) &:= \frac{\partial^2}{\partial \theta \partial t} \psi_\theta(t). \end{aligned} \tag{B.1}$$

eq:notation

The expression for these derivatives for Clayton and Gumbel generators are provided in Table B.1. Note that the higher-order derivatives of $\psi_\theta(t)$ with respect to t involve the falling factorial function $(x)_n := \sum_{j=1}^n x^j s(n, j)$ and the function $s_{nk}(x) := \sum_{j=k}^n x^j s(n, j) S(j, k)$, where $s(n, k)$ and $S(n, k)$ are Stirling numbers of the first and second kind (Goldberg et al., 1972, Sections 24.1.3-4). These functions and their derivatives are given explicitly in Table B.2. Derivatives of multi-parameter functions are defined similarly

$$\begin{aligned} \dot{t}(\mathbf{u}) &:= \frac{\partial}{\partial \theta_0} t(\mathbf{u}), & \dot{t}_s(\mathbf{u}) &:= \frac{\partial}{\partial \theta_s} t(\mathbf{u}), & \dot{\dot{t}}(\mathbf{u}) &:= \frac{\partial^2}{\partial \theta_0 \partial \theta_0} t(\mathbf{u}), \\ \overset{sr}{t}(\mathbf{u}) &:= \frac{\partial}{\partial \theta_s \partial \theta_r} t(\mathbf{u}), & \overset{\circ s}{t}(\mathbf{u}) &:= \frac{\partial}{\partial \theta_0 \partial \theta_s} t(\mathbf{u}). \end{aligned} \tag{B.2}$$

eq:notation

Following Theorem 3.3 of Hofert and Pham (2013), if $\phi_0 \circ \psi_i$ ($i = 0, \dots, K$) have completely monotone first-order derivatives, the density c associated to a HAC C (whose generators are com-

pletely monotone) have the general form,

$$c(\mathbf{u}) = \left\{ \sum_{k=K}^d B_k(\mathbf{u}) \Psi_k(\mathbf{u}) \right\} \prod_{i=1}^K \prod_{j=1}^{d_i} \phi'_i(u_{ij}), \quad B_k(\mathbf{u}) := b_k(\mathbf{t}(\mathbf{u})), \quad \Psi_k(\mathbf{u}) := \psi_0^{(k)}(\mathbf{t}(\mathbf{u})), \quad (\text{B.3})$$

for $\mathbf{u} \in (0, 1)^d$, where for any $\mathbf{t} \in (0, \infty)^K$, $b_k(\mathbf{t})$ is given by

$$b_k(\mathbf{t}) = \sum_{\mathbf{q} \in \mathcal{Q}_{d,k}} \prod_{i=1}^K a_{iq_i}(t_i), \quad (\text{B.4})$$

with $\mathcal{Q}_{d,k} = \{\mathbf{q} \in \mathbb{N}^K : \sum_{i=1}^K q_i = k, q_i \leq d_i, i \in \{1, \dots, K\}\}$ and a_{iq_i} as in (Hofert and Pham, 2013, Eq. (12)). In general, the functions a_{iq_i} ($i = 1, \dots, d_0$) have complicated expressions in terms of Bell polynomials, but for Clayton and Gumbel generators, they simplify significantly to

$$a_{iq_i}(t) := (\gamma^{\theta_i} + t)^{q_i \theta_0 / \theta_i - d_i} s_{d_i q_i}(\theta_0 / \theta_i), \quad (\text{B.5})$$

where $\gamma = 1$ for the Clayton generator and $\gamma = 0$ for the Gumbel generator. Note that a_{iq_i} depends on θ_i , and hence b_k depends on $\boldsymbol{\theta}$ as well. The derivatives of $a_{ij}(t)$ and $A_{ij}(\mathbf{u}) := a_{ij}\{\mathbf{t}(\mathbf{u}_i)\}$ are given in Tables B.3 and B.4, respectively, while the derivatives of $B_k(\mathbf{u})$ are given in Table B.5.

Remark 4. The general form of the function a_{iq_i} in (B.5) is obtained from the fact that both the Clayton and Gumbel families are subsets of the tilted outer power family; see Hofert (2010) and (Hofert and Pham, 2013, Section 4.1). This family is characterized by generators ψ_θ of the form $\psi_\theta(t) = \psi_*\{(\gamma^\theta + t)^{1/\theta} - \gamma\}$ for $\gamma \in [0, \infty)$, $\theta \in [1, \infty)$ and a ∞ -monotone generator ψ_* . The Clayton generator is recovered by setting $\psi_*(t) = 1/(1+t)$ and $\gamma = 1$, and the Gumbel generator is recovered by setting $\psi_*(t) = e^{-t}$ and $\gamma = 0$.

B.2 Partial derivatives of the log-likelihood

We now discuss how the first- and second-order partial derivatives of the log-likelihood of HACs are obtained. The expression for the second-order derivatives provides an estimator for the Fisher information matrix \mathbf{J}_θ which appeared in Section 4 via the second Bartlett identity. In view of (B.3), one can write the HAC log-density as $\ln c(\mathbf{u}) = \ln \mathfrak{B}_1(\mathbf{u}) + \ln \mathfrak{B}_2(\mathbf{u})$, where

$$\mathfrak{B}_1 \equiv \mathfrak{B}_1(\mathbf{u}) = (-1)^d \sum_{k=K}^d B_k(\mathbf{u}) \Psi_k(\mathbf{u}) \quad \text{and} \quad \mathfrak{B}_2 \equiv \mathfrak{B}_2(\mathbf{u}) = \prod_{i=1}^K \prod_{j=1}^{d_i} (-1) \phi'_i(u_{ij}). \quad (\text{B.6})$$

In particular, for each $i = 0, \dots, K$,

$$\frac{\partial \ln c(\mathbf{u})}{\partial \theta_s} = \sum_{k=1}^2 \frac{\partial \ln \mathfrak{B}_k}{\partial \theta_s} = \sum_{k=1}^2 \left(\frac{\partial \mathfrak{B}_k}{\partial \theta_s} \right) \mathfrak{B}_k^{-1}$$

and

$$\frac{\partial^2 \ln c(\mathbf{u})}{\partial \theta_s \partial \theta_r} = \sum_{k=1}^2 \left\{ \left(\frac{\partial^2 \mathfrak{B}_k}{\partial \theta_s \partial \theta_r} \right) \mathfrak{B}_k^{-1} - \left(\frac{\partial \mathfrak{B}_k}{\partial \theta_s} \right) \left(\frac{\partial \mathfrak{B}_k}{\partial \theta_r} \right) \mathfrak{B}_k^{-2} \right\}.$$

It is straightforward to verify that $\partial \mathfrak{B}_2 / \partial \theta_0 = 0$, and thus also that $\partial^2 \mathfrak{B}_2 / (\partial \theta_0 \partial \theta_i) = 0$ for all $i = 0, \dots, K$. For Clayton and Gumbel generators, $\partial \ln \mathfrak{B}_2 / \partial \theta_i = d_i / \theta_i + \sum_{j=1}^{d_i} g(u_{ij})$ and $\partial^2 \mathfrak{B}_2 / \partial \theta_i^2 = -d_i / \theta_i^2$, where $g(u_{ij}) = -\ln(u_{ij})$ for the Clayton generator and $g(u_{ij}) = \ln\{-\ln(u_{ij})\}$ for the Gumbel generator.

The partial derivatives of \mathfrak{B}_1 are given by

$$\begin{aligned} \frac{\partial \mathfrak{B}_1}{\partial \theta_s} &= (-1)^d \sum_{k=d_0}^d \left\{ \Psi_k \overset{s}{B}_k + B_k \overset{s}{\Psi}_k \right\} \\ \frac{\partial^2 \mathfrak{B}_1}{\partial \theta_s \partial \theta_r} &= (-1)^d \sum_{k=d_0}^d \left\{ \overset{sr}{B}_k \Psi_k + \overset{s}{B}_k \overset{r}{\Psi}_k + \overset{r}{B}_k \overset{s}{\Psi}_k + B_k \overset{sr}{\Psi}_k \right\}, \end{aligned} \tag{B.7}$$

eq:derivati

where the dependence of each term on \mathbf{u} has been suppressed for convenience. Explicit expressions for the Clayton and Gumbel families based on these formulas can be constructed from Tables B.5 and B.6, which themselves builds upon previous tables and definitions.

Along with Tables B.1–B.6, the equations in (B.6) and (B.7) contain the necessary material for implementing functions that returns the log-likelihood and its partial derivatives. As part of the Supplementary Material accompanying this article, we provide our own implementations written in the R programming language for calculating these derivatives. In the simulations of §5, we use these to assess the accuracy of numerical estimations of Σ , and generally rely on the more efficient estimation functions available in the R package HAC (Okhrin and Ristig, 2014).

Table B.1: Derivatives of the generator ψ_θ and its inverse ϕ_θ relevant for computing Clayton and Gumbel HAC densities and their associated Fisher information. See (B.1)–(B.2) for notation.

	Clayton	Gumbel
$\psi_\theta(t)$	$(1+t)^{-1/\theta}$	$\exp(-t^{1/\theta})$
$\psi'_\theta(t)$	$-(1/\theta)(1+t)^{-1/\theta-1}$	$-\psi_\theta(t)t^{1/\theta-1}(1/\theta)$
$\psi_\theta^{(k)}(t)$	$(-1/\theta)_k(1+t)^{-1/\theta-k}$	$\psi_\theta(t)\sum_{j=1}^k t^{j/\theta-k}(-1)^j s_{kj}(1/\theta)$
$\dot{\psi}_\theta(t)$	$\psi_\theta(t)\ln(1+t)/\theta^2$	$\psi_\theta(t)t^{1/\theta}\ln(t)/\theta^2$
$\ddot{\psi}_\theta(t)$	$\dot{\psi}_\theta(t)[\ln(1+t)/\theta^2 - 2/\theta]$	$\dot{\psi}_\theta(t)[(t^{1/\theta} - 1)\ln(t)/\theta^2 - 2/\theta]$
$\dot{\psi}'_\theta(t)$	$\psi'_\theta(t)[\ln(1+t)/\theta^2 - 1/\theta]$	$\psi'_\theta(t)[(t^{1/\theta} - 1)\ln(t)/\theta^2 - 1/\theta]$
$\phi_\theta(u)$	$u^{-\theta} - 1$	$(-\ln u)^\theta$
$\phi'_\theta(u)$	$-\theta u^{-\theta-1}$	$-\theta u^{-1}(-\ln u)^{\theta-1}$
$\phi_\theta^{(2)}(u)$	$-\phi'_\theta(u)(\theta+1)u^{-1}$	$\phi'_\theta(u)u^{-1}[(\theta-1)/\ln(u) - 1]$
$\dot{\phi}_\theta(u)$	$u^{-\theta}\ln(1/u)$	$\phi_\theta(u)\ln(-\ln u)$
$\ddot{\phi}_\theta(u)$	$\dot{\phi}_\theta(u)\ln(1/u)$	$\dot{\phi}_\theta(u)\ln(-\ln u)$
$\dot{\phi}'_\theta(u)$	$\phi'_\theta(u)[1/\theta - \ln(u)]$	$\phi'_\theta(u)[1/\theta - \ln(-\ln u)]$

Table B.2: Functions involving Stirling numbers of the first and second kind (Goldberg et al., 1972, Sections 24.1.3-4), denoted s and S , respectively, and their derivatives appearing in HAC densities and their associated Fisher information. See (B.1)–(B.2) for notation.

$s_{nk}(x)$	$\sum_{j=k}^n x^j s(n, j)S(j, k)$	$(x)_n$	$\sum_{j=1}^n x^j s(n, j)$
$s'_{nk}(x)$	$\sum_{j=k}^n j x^{j-1} s(n, j)S(j, k)$	$(x)'_n$	$\sum_{j=1}^n j x^{j-1} s(n, j)$
$s_{nk}^{(2)}(x)$	$\sum_{j=k}^n j(j-1)x^{j-2} s(n, j)S(j, k)$	$(x)_n^{(2)}$	$\sum_{j=1}^n j(j-1)x^{j-2} s(n, j)$

Table B.3: The function a_{sj} of (B.5) and its derivatives appearing in Clayton ($\gamma = 1$) and Gumbel ($\gamma = 0$) HAC densities and their associated Fisher information. See (B.1)–(B.2) for notation.

:a-function

$\xi_{sj}(t)$	$:= (\gamma^{\theta_s} + t)^{j\theta_0/\theta_s - d_s}$	$\zeta_s(t)$	$:= \frac{j}{\theta_s} \ln(\gamma^{\theta_s} + t)$
$a_{sj}(t)$	$\xi_{sj}(t) s_{d_{sj}}(\frac{\theta_0}{\theta_s})$		
$a'_{sj}(t)$	$(j\theta_0/\theta_s - d_s)(\gamma^{\theta_s} + t)^{-1} a_{sj}(t)$		
$a_{sj}^{(2)}(t)$	$(j\theta_0/\theta_s - d_s - 1)(\gamma^{\theta_s} + t)^{-1} a'_{sj}(t)$		
$\overset{\circ}{a}_{sj}(t)$	$\zeta_s(t) a_{sj}(t) + \xi_{sj}(t) s'_{d_{sj}}(\frac{\theta_0}{\theta_s}) \frac{1}{\theta_s}$		
$\overset{s}{a}_{sj}(t)$	$\frac{-\theta_0}{\theta_s} \zeta_s(t) a_{sj}(t) - \xi_{sj}(t) s'_{d_{sj}}(\frac{\theta_0}{\theta_s}) \frac{\theta_0}{\theta_s^2}$		
$\overset{\circ}{a}'_{sj}(t)$	$(\gamma^{\theta_s} + t)^{-1} \left[\frac{j}{\theta_s} a_{sj}(t) + (j\theta_0/\theta_s - d_s) \overset{\circ}{a}_{sj}(t) \right]$		
$\overset{s}{a}'_{sj}(t)$	$(\gamma^{\theta_s} + t)^{-1} \left[\frac{-j\theta_0}{\theta_s^2} a_{sj}(t) + (j\theta_0/\theta_s - d_s) \overset{s}{a}_{sj}(t) \right]$		
$\overset{\circ\circ}{a}_{sj}(t)$	$\zeta_s(t) \left[\frac{\partial}{\partial \theta_0} a_{sj}(t) + \xi_{sj}(t) s'_{d_{sj}}(\frac{\theta_0}{\theta_s}) \frac{1}{\theta_s} \right] + \xi_{sj}(t) s_{d_{sj}}^{(2)}(\frac{\theta_0}{\theta_s}) \frac{1}{\theta_s^2}$		
$\overset{s}{a}_{sj}(t)$	$\frac{\theta_0 \zeta_s(t)}{\theta_s} \left[\frac{2}{\theta_s} a_{sj}(t) - \overset{s}{a}_{sj}(t) \right] + \frac{\theta_0^2 \xi_{sj}(t)}{\theta_s^4} \left\{ \theta_s \left[\zeta_s(t) + \frac{2}{\theta_0} \right] s'_{d_{sj}}(\frac{\theta_0}{\theta_s}) + s_{d_{sj}}^{(2)}(\frac{\theta_0}{\theta_s}) \right\}$		

Table B.4: The function A_{sj} defined below (B.5) and its derivatives appearing in HAC densities and their associated Fisher information. See (B.1)–(B.2) for notation.

:A-function

$A_{sj}(\mathbf{u})$	$a_{sj}(t_s)$	$t_s \equiv t(\mathbf{u}_s) := \sum_{j=1}^{d_s} \psi_{\theta_s}(u_{sj})$
$\overset{\circ}{A}_{sj}(\mathbf{u})$	$\overset{\circ}{a}_{sj}(t_s)$	$\dot{t}_s \equiv \dot{t}_s(\mathbf{u}_s) := \sum_{j=1}^{d_s} \dot{\psi}_{\theta_s}(u_{sj})$
$\overset{s}{A}_{sj}(\mathbf{u})$	$\overset{s}{a}_{sj}(t_s) + \dot{t}_s \overset{s}{a}'_{sj}(t_s)$	$\ddot{t}_s \equiv \ddot{t}_s(\mathbf{u}_s) := \sum_{j=1}^{d_s} \ddot{\psi}_{\theta_s}(u_{sj})$
$\overset{\circ\circ}{A}_{sj}(\mathbf{u})$	$\overset{\circ\circ}{a}_{sj}(t_s)$	
$\overset{\circ s}{A}_{sj}(\mathbf{u})$	$\overset{\circ s}{a}_{sj}(t_s) + \dot{t}_s \overset{\circ s}{a}'_{sj}(t_s)$	
$\overset{ss}{A}_{sj}(\mathbf{u})$	$\overset{ss}{a}_{sj}(t_s) + 2 \overset{s}{a}'_{sj}(t_s) \dot{t}_s + \ddot{t}_s \overset{ss}{a}''_{sj}(t_s) (\dot{t}_s)^2 + \overset{s}{a}'_{sj}(t_s)$	

Table B.5: The function $B_k := b_k \circ \mathbf{t}$ defined in (B.3)–(B.4) and its derivatives appearing in HAC densities and their associated Fisher information. See (B.1)–(B.2) for notation.

$A_{sj_s} := a_{sj_s}(t_s)$	$t_s \equiv t(\mathbf{u}_s) := \sum_{j=1}^{d_s} \psi_{\theta_s}(u_{sj})$
$\mathcal{S} := \{1, \dots, d_0\}$	$\mathcal{S}_s := \mathcal{S} \setminus \{s\} \quad \mathcal{S}_{sr} := \mathcal{S} \setminus \{s, r\}$

$B_k(\mathbf{u})$	$\sum_{j \in \mathcal{Q}_{d,k}} \prod_{s \in \mathcal{S}} a_{sj_s}$
$\overset{\circ}{B}_k(\mathbf{u})$	$\sum_{j \in \mathcal{Q}_{d,k}} \sum_{s \in \mathcal{S}} \left\{ \left[\prod_{m \in \mathcal{S}_s} a_{mj_m}(t_m) \right] \overset{\circ}{A}_{sj_s} \right\}$
$\overset{\dot{s}}{B}_k(\mathbf{u})$	$\sum_{j \in \mathcal{Q}_{d,k}} \left[\prod_{m \in \mathcal{S}_s} a_{mj_m}(t_m) \right] \overset{\dot{s}}{A}_{sj_s}$
$\overset{\circ\circ}{B}_k(\mathbf{u})$	$\sum_{j \in \mathcal{Q}_{d,k}} \sum_{s \in \mathcal{S}} \left(\left\{ \sum_{l \in \mathcal{S}_s} \overset{\circ}{A}_{lj_l} \prod_{m \in \mathcal{S}_{sl}} a_{mj_m}(t_m) \right\} \overset{\circ}{a}_{sj_s} + \left[\prod_{m \in \mathcal{S}_s} a_{mj_m}(t_m) \right] \overset{\circ\circ}{a}_{sj_s} \right)$
$\overset{\circ\dot{s}}{B}_k(\mathbf{u})$	$\sum_{j \in \mathcal{Q}_{d,k}} \left(\left\{ \sum_{l \in \mathcal{S}_s} \left[\prod_{m \in \mathcal{S}_{sl}} a_{mj_m}(t_m) \right] \overset{\circ}{a}_{lj_l} \right\} \overset{\dot{s}}{A}_{sj_s} + \left[\prod_{m \in \mathcal{S}_s} a_{mj_m}(t_m) \right] \overset{\circ\dot{s}}{A}_{sj_s} \right)$
$\overset{ss}{B}_k(\mathbf{u})$	$\sum_{j \in \mathcal{Q}_{d,k}} \left[\prod_{m \in \mathcal{S}_s} a_{mj_m}(t_m) \right] \overset{ss}{A}_{sj_s}$
$\overset{sm}{B}_k(\mathbf{u})$	$\sum_{j \in \mathcal{Q}_{d,k}} \left[\prod_{l \in \mathcal{S}_{sm}} a_{lj_l}(t_l) \right] \overset{\dot{s}}{A}_{sj_s} \overset{m}{A}_{mj_m}$

Table B.6: The function $\Psi_k := \psi_0^{(k)} \circ t$ defined in (B.3) and its derivatives appearing in Clayton and Gumbel HAC densities and their associated Fisher information. See (B.1)–(B.2) for notation.

Clayton: $f_{\theta k}(x) = (-\frac{1}{\theta})_k (1+x)^{-(k+1/\theta)}$	Gumbel: $f_{\theta k}(x) = \psi_{\theta}(x) \sum_{j=1}^k x^{j/\theta - k} (-1)^j s_{kj}(1/\theta)$
--	--

$\Psi_k(\mathbf{u})$	$f_{\theta_0 k}(t)$	$t \equiv t(\mathbf{u}) = \sum_{i=1}^K \phi_0(C_i(\mathbf{u}_i))$
$\overset{\circ}{\Psi}_k(\mathbf{u})$	$\overset{\circ}{f}_{\theta_0 k}(t) + \overset{\circ}{t} \overset{\circ}{f}'_{\theta_0 k}(t)$	$\overset{\circ}{t} \equiv \overset{\circ}{t}(\mathbf{u}) = \sum_{i=1}^K \dot{\phi}_0(C_i(\mathbf{u}_i))$
$\overset{\dot{s}}{\Psi}_k(\mathbf{u})$	$\overset{\dot{s}}{t} \overset{\dot{s}}{f}'_{\theta_0 k}(t)$	$\overset{\dot{s}}{t} \equiv \overset{\dot{s}}{t}(\mathbf{u}) = \phi'_0(C_s(\mathbf{u}_s)) \dot{C}_s(\mathbf{u}_s)$
$\overset{\circ\circ}{\Psi}_k(\mathbf{u})$	$\overset{\circ\circ}{f}_{\theta_0 k}(t) + \overset{\circ}{t} \overset{\circ\circ}{f}'_{\theta_0 k}(t) + \left(\overset{\circ}{t} \right)^2 \overset{\circ\circ}{f}''_{\theta_0 k}(t) + \overset{\circ\circ}{t} \overset{\circ\circ}{f}'_{\theta_0 k}(t)$	$\overset{\circ\circ}{t} \equiv \overset{\circ\circ}{t}(\mathbf{u}) = \sum_{i=1}^K \ddot{\phi}_0(C_i(\mathbf{u}_i))$
$\overset{\circ\dot{s}}{\Psi}_k(\mathbf{u})$	$\overset{\circ\dot{s}}{t} \overset{\circ\dot{s}}{f}'_{\theta_0 k}(t) + \overset{\circ}{t} \overset{\circ\dot{s}}{t} \overset{\circ\dot{s}}{f}''_{\theta_0 k}(t) + \overset{\circ\dot{s}}{t} \overset{\circ\dot{s}}{f}'_{\theta_0 k}(t)$	$\overset{\circ\dot{s}}{t} \equiv \overset{\circ\dot{s}}{t}(\mathbf{u}) = \dot{\phi}'_0(C_s(\mathbf{u}_s)) \dot{C}_s(\mathbf{u}_s)$
$\overset{ss}{\Psi}_k(\mathbf{u})$	$\left(\overset{\circ}{t} \right)^2 \overset{ss}{f}''_{\theta_0 k}(t) + \overset{ss}{t} \overset{ss}{f}'_{\theta_0 k}(t)$	$\overset{ss}{t} \equiv \overset{ss}{t}(\mathbf{u}) = \phi''_0(C_s(\mathbf{u}_s)) \{ \dot{C}_s(\mathbf{u}_s) \}^2 + \phi'_0(C_s(\mathbf{u}_s)) \ddot{C}_s(\mathbf{u}_s)$
$\overset{sm}{\Psi}_k(\mathbf{u})$	$\overset{\circ}{t} \overset{m}{t} \overset{m}{f}'_{\theta_0 k}(t)$	

C Example: trivariate Clayton HAC

app:Clayton

To demonstrate the relatively weak nature of the non-singularity of the Fisher information matrix and the Lipschitz condition in Assumptions B, consider the trivariate Clayton HAC model given by

$$C_{\boldsymbol{\theta}}(\mathbf{u}) = C_{\theta_0}(C_{\theta_1}(u_1, u_2), u_3) = \left\{ (u_{11}^{-\theta_1} + u_{12}^{-\theta_1} - 1)^{\theta_0/\theta_1} + u_{21}^{-\theta_0} - 1 \right\}^{-1/\theta_0}, \quad \theta_0, \theta_1 \in \Theta = (0, \infty),$$

which satisfies Assumptions A. The derivations which follows can be extended to arbitrary Clayton HACs, although the notation quickly becomes cumbersome. To check the non-singularity of the Fisher information, we computed the latter's determinant, using the numerical method described in §4, for each value of $\boldsymbol{\theta}$ on a fine grid covering $\{(x_0, x_1) \in (0, 2] : x_0 \leq x_1\}$. The results are depicted in Figure 3, which shows that the determinant is positive for all values of $\boldsymbol{\theta}$ on the grid, suggesting that this is likely to hold for the entire parameter space. Furthermore, we note that as the copula density is infinitely differentiable, it is trivially differentiable in quadratic mean.

It only remains to verify the Lipschitz condition in Assumption B. We decompose the log-likelihood function into a sum of 5 functions, which individually satisfy the Lipschitz assumption. Specifically, we upper bound the absolute value of the difference of each function within a small neighborhood by a term of the kind $\|\boldsymbol{\theta}' - \boldsymbol{\vartheta}\|f(u)$, we then combine these upper bounds together through the triangle inequality and further demonstrate that these functions satisfy the square integrability condition. The following holds for all $\boldsymbol{\theta}'$ such that $\|\boldsymbol{\theta}' - \boldsymbol{\vartheta}\|_2 < \epsilon(\boldsymbol{\vartheta})$ and for $\epsilon(\boldsymbol{\vartheta}) = \min(\vartheta_1/2, \vartheta_0/2)$; these quantities only depend on the true data generating parameter $\boldsymbol{\vartheta}$. The copula density can be written as:

$$\begin{aligned} c_{\boldsymbol{\theta}}(u_{11}, u_{12}, u_{21}) &= -\theta_1^2 (u_{11} u_{12})^{-(1+\theta_1)} \theta_0 u_{21}^{-(1+\theta_0)} \left\{ \left(1 + t_1(u_{11}, u_{12})\right)^{\frac{\theta_0}{\theta_1} - 2} s_{21}\left(\frac{\theta_0}{\theta_1}\right) \left(\frac{1}{\theta_0} + \frac{1}{\theta_0^2}\right) C_{\boldsymbol{\theta}}(u_{11}, u_{12}, u_{21})^{2\theta_0+1} \right. \\ &\quad \left. - \left(1 + t_1(u_{11}, u_{12})\right)^{\frac{2\theta_0}{\theta_1} - 2} s_{22}\left(\frac{\theta_0}{\theta_1}\right) \left(\frac{1}{\theta_0} + \frac{1}{\theta_0^2}\right) \left(2 + \frac{1}{\theta_0}\right) C_{\boldsymbol{\theta}}(u_{11}, u_{12}, u_{21})^{3\theta_0+1} \right\} \\ &= \underbrace{\theta_1^2 (u_{11} u_{12})^{-(1+\theta_1)} \theta_0 u_{21}^{-(1+\theta_0)}}_{A(\boldsymbol{\theta}, \mathbf{u})} \underbrace{\left\{ C_{\boldsymbol{\theta}}(u_{11}, u_{12}, u_{21})^{2\theta_0+1} \right\}}_{B(\boldsymbol{\theta}, \mathbf{u})} \underbrace{\left\{ \left(1 + t_1(u_{11}, u_{12})\right)^{\frac{\theta_0}{\theta_1} - 2} \right\}}_{C(\boldsymbol{\theta}, \mathbf{u})} \\ &\quad \times \underbrace{\left(\frac{1}{\theta_0} + \frac{1}{\theta_0^2}\right)}_{D(\boldsymbol{\theta}, \mathbf{u})} \times \underbrace{\left\{ s_{21}\left(\frac{\theta_0}{\theta_1}\right) - \left(1 + t_1(u_{11}, u_{12})\right)^{\frac{\theta_0}{\theta_1}} s_{22}\left(\frac{\theta_0}{\theta_1}\right) \left(2 + \frac{1}{\theta_0}\right) C_{\boldsymbol{\theta}}(u_{11}, u_{12}, u_{21})^{\theta_0} \right\}}_{E(\boldsymbol{\theta}, \mathbf{u})} \end{aligned}$$

where,

$$C_{\boldsymbol{\theta}}(u_{11}, u_{12}, u_{21}) = \left\{ \left(u_{11}^{-\theta_1} + u_{12}^{-\theta_1} - 1 \right)^{\frac{\theta_0}{\theta_1}} + u_{21}^{-\theta_0} - 1 \right\}^{\frac{-1}{\theta_0}},$$

and $s_{11}(\cdot)$ and $s_{12}(\cdot)$, are polynomials whose form are given in Appendix A.

Controlling $\ln(A(\boldsymbol{\theta}, \mathbf{u}))$. Consider:

$$|\ln(A(\boldsymbol{\theta}', \mathbf{u})) - \ln(A(\boldsymbol{\vartheta}, \mathbf{u}))| = |2\{\ln(\theta'_1) - \ln(\vartheta_1)\} + \{\ln(\theta'_0) - \ln(\vartheta_0)\}|$$

$$+(\vartheta_1 - \theta'_1) \ln(u_{11}u_{12}) + (\vartheta_0 - \theta'_0) \ln(u_{21})|,$$

applying the triangle inequality, we see that the differences in logarithms:

$$2 |\ln(\vartheta_1) - \ln(\theta'_1)| \leq \frac{|\vartheta_1 - \theta'_1|}{\vartheta_1 - \epsilon_1},$$

by a first-order Taylor expansion and any this is valid for any $0 < \epsilon_1 \leq \theta_1/2$. As for

$$|(\vartheta_1 - \theta'_1) \ln(u_{11}u_{12})| \leq |(\vartheta_1 - \theta'_1)| \ln(u_{11}u_{12}) \leq 2^{1/2} \|\boldsymbol{\theta}' - \boldsymbol{\vartheta}\|_2 \ln(u_{11}u_{12})$$

The other differences are bounded by similar terms which only involves constants and logarithms of u_{11}, u_{12}, u_{21} .

Controlling $\ln(B(\boldsymbol{\theta}, \mathbf{u}))$. Consider the derivative:

$$\begin{aligned} \left| \frac{\partial}{\partial \theta} \ln(B(\boldsymbol{\theta}, \mathbf{u})) \right| &= \left| \frac{2}{\theta_0^2} \ln\{(u_{11}^{-\theta_1} + u_{12}^{-\theta_1} - 1)^{\theta_0/\theta_1} + u_{21}^{-\theta_0} - 1\} \right. \\ &\quad \left. + \frac{1}{\theta_0} \left(1 - \frac{2}{\theta_0}\right) \frac{(u_{11}^{-\theta_1} + u_{12}^{-\theta_1} - 1)^{\theta_0/\theta_1} \ln(u_{11}^{-\theta_1} + u_{12}^{-\theta_1} - 1) + u_{21}^{-\theta_0} \ln(u_{21}^{-\theta_0})}{(u_{11}^{-\theta_1} + u_{12}^{-\theta_1} - 1) + u_{21}^{-\theta_0} - 1} \right| \\ &\leq \left| \frac{2}{\theta_0^2} \ln\{u_{11}^{-\theta_1} + u_{12}^{-\theta_1} + u_{21}^{-\theta_0}\} + \frac{1}{\theta_0} \left(1 + \frac{2}{\theta_0}\right) \ln(u_{11}^{-\theta_1} + u_{12}^{-\theta_1}) + \ln(u_{21}^{-\theta_0}) \right|, \end{aligned}$$

as $\theta_0/\theta_1 \leq 1$, $\ln(\cdot)$ is a monotonic function and $0 < x/(x+y) \leq 1$ for positive x and y . While the partial derivative with respect to θ_1 :

$$\left| \frac{\partial}{\partial \theta_1} \ln(B(\boldsymbol{\theta}, \mathbf{u})) \right| \leq (1 + 2/\theta_0) \left\{ \frac{\theta_0}{\theta_1} (\ln(u_{11}^{-1}) + \ln(u_{12}^{-1})) + \frac{\theta_0}{\theta_1^2} \ln(u_{11}^{-\theta_1} + u_{12}^{-\theta_1}) \right\},$$

through similar calculations. These derivatives are bounded within the chosen radius around $\boldsymbol{\vartheta}$, therefore these upper bounds may be used as the Lipchitz constant.

Controlling $\ln(C(\boldsymbol{\theta}, \mathbf{u}))$. Consider:

$$\begin{aligned} &|\ln(C(\boldsymbol{\theta}', \mathbf{u})) - \ln(C(\boldsymbol{\vartheta}, \mathbf{u}))| \\ &\leq \left| \frac{\theta'_0}{\theta'_1} - \frac{\vartheta_0}{\vartheta_1} \right| \ln\left(1 + t_1^{\vartheta}(u_{11}, u_{12})\right) + \left| \frac{\vartheta_0}{\vartheta_1} - 2 \right| \left| \ln\left(1 + t_1^{\vartheta}(u_{11}, u_{12})\right) - \ln\left(1 + t_1^{\theta'_0}(u_{11}, u_{12})\right) \right| \\ &\leq \frac{\vartheta_1 |\vartheta_0 - \theta'_0| + \vartheta_0 |\vartheta_1 - \theta'_1|}{\vartheta_1 (\vartheta_1 - \epsilon_1)} \ln(u_{11}^{-\vartheta_1} + u_{11}^{-\vartheta_1}) + |\theta'_1 - \vartheta_1| \left| \frac{\vartheta_0}{\vartheta_1} - 2 \right| \left| \ln(u_{11}^{-1}) + \ln(u_{12}^{-1}) \right| \\ &\leq \|\boldsymbol{\theta}' - \boldsymbol{\vartheta}\|_2 \left[\frac{\sqrt{2} \max(\vartheta_0, \vartheta_1)}{\vartheta_1 (\vartheta_1 - \epsilon_1)} \ln(u_{11}^{-\vartheta_1} + u_{11}^{-\vartheta_1}) + \sqrt{2} \left| \frac{\vartheta_0}{\vartheta_1} - 2 \right| \left| \ln(u_{11}^{-1}) + \ln(u_{12}^{-1}) \right| \right], \end{aligned}$$

where we have used the following first-order Taylor expansion, for every u_{11} and u_{12} fixed

$$\begin{aligned} & \left| \ln \left(1 + t_1^{\vartheta}(u_{11}, u_{12}) \right) - \ln \left(1 + t_1^{\vartheta'}(u_{11}, u_{12}) \right) \right| \\ &= |\theta'_1 - \vartheta_1| \left\{ \frac{u_{12}^{\tilde{\theta}} \ln(u_{11}^{-1}) + u_{11}^{\tilde{\theta}} \ln(u_{12}^{-1})}{u_{11}^{\tilde{\theta}} + u_{12}^{\tilde{\theta}} - 1} \right\} \leq \ln(u_{11}^{-1}) + \ln(u_{12}^{-1}), \end{aligned}$$

where $\tilde{\theta}$ lies between θ'_1 and ϑ_1 . Similar to the previous case, these derivatives are bounded within the chosen radius around ϑ and can therefore be used as the Lipchitz constant.

Controlling $\ln(D(\boldsymbol{\theta}, \mathbf{u}))$. Consider:

$$\ln(D(\boldsymbol{\theta}, \mathbf{u})) = \ln \left(\frac{1}{\theta_1} + \frac{1}{\theta_1^2} \right).$$

Using a first-order Taylor expansion we have for some $\tilde{\theta}$ between θ'_1 and ϑ_1 :

$$\left| \ln \left(\frac{1}{\theta'_1} + \frac{1}{(\theta'_1)^2} \right) - \ln \left(\frac{1}{\vartheta_1} + \frac{1}{\vartheta_1^2} \right) \right| \leq \frac{1}{\tilde{\theta}} \frac{1 + 2\tilde{\theta}^{-2}}{1 + \tilde{\theta}^{-1}} |\theta_1 - \theta'_1| \leq \frac{|\vartheta_1 - \theta'_1|}{\vartheta_0 - \epsilon}.$$

Controlling $\ln(E(\boldsymbol{\theta}, \mathbf{u}))$.

$$\begin{aligned} \ln(E(\boldsymbol{\theta}, \mathbf{u})) &= \ln \left[-s_{11} \left(\frac{\theta_0}{\theta_1} \right) + \left(1 + t_1(u_{11}, u_{12}) \right)^{\frac{\theta_0}{\theta_1}} s_{22} \left(\frac{\theta_0}{\theta_1} \right) \left(2 + \frac{1}{\theta_0} \right) C_{\boldsymbol{\theta}}(u_{11}, u_{12}, u_{21})^{\theta_0} \right] \\ &= \ln \left[\left(\frac{\theta_1}{\theta_0} - 1 \right) + \frac{\left(u_{11}^{-\theta_1} + u_{12}^{-\theta_1} - 1 \right)^{\frac{\theta_0}{\theta_1}}}{\left\{ \left(u_{11}^{-\theta_1} + u_{12}^{-\theta_1} - 1 \right)^{\frac{\theta_0}{\theta_1}} + u_{21}^{-\theta_0} - 1 \right\}} \left(2 + \frac{1}{\theta_0} \right) \right] + \ln \left(\frac{\theta_0^2}{\theta_1^2} \right) \end{aligned}$$

We show that the derivative of this function with respect to θ_0 and θ_1 is bounded within the chosen neighborhood of ϑ . Let:

$$\begin{aligned} W(\boldsymbol{\theta}, \mathbf{u}) &:= \frac{\left(u_{11}^{-\theta_1} + u_{12}^{-\theta_1} - 1 \right)^{\frac{\theta_0}{\theta_1}}}{\left\{ \left(u_{11}^{-\theta_1} + u_{12}^{-\theta_1} - 1 \right)^{\frac{\theta_0}{\theta_1}} + u_{21}^{-\theta_0} - 1 \right\}}, \\ V(\boldsymbol{\theta}, \mathbf{u}) &:= \frac{u_{21}^{-\theta_0}}{\left\{ \left(u_{11}^{-\theta_1} + u_{12}^{-\theta_1} - 1 \right)^{\frac{\theta_0}{\theta_1}} + u_{21}^{-\theta_0} - 1 \right\}}, \\ Z(\boldsymbol{\theta}, \mathbf{u}) &= \frac{\theta_0}{\theta_1} \left\{ \frac{u_{11}^{-\theta_1} \ln(u_{11}^{-1}) + u_{12}^{-\theta_1} \ln(u_{12}^{-1})}{u_{11}^{-\theta_1} + u_{12}^{-\theta_1} - 1} - \frac{\ln(u_{11}^{-\theta_1} + u_{12}^{-\theta_1} - 1)}{\theta_1} \right\}. \end{aligned}$$

Note $W(\boldsymbol{\theta}, \mathbf{u})$ and $V(\boldsymbol{\theta}, \mathbf{u})$ are positive and bounded by 1. The partial derivatives are:

$$\begin{aligned} \left| \frac{\partial}{\partial \theta_0} \ln(E(\boldsymbol{\theta}, \mathbf{u})) \right| &= \left| \left\{ -\frac{1}{\theta_0^2} W(\boldsymbol{\theta}, \mathbf{u}) + \frac{2 + \theta_0^{-1}}{\theta_1} W(\boldsymbol{\theta}, \mathbf{u}) \ln(u_{11}^{-\theta_1} + u_{12}^{-\theta_1} - 1) - \frac{\theta_1}{\theta_0^2} \right. \right. \\ &\quad \left. \left. - \left(2 + \frac{1}{\theta_0} \right) W(\boldsymbol{\theta}, \mathbf{u}) \left\{ \theta_1^{-1} W(\boldsymbol{\theta}, \mathbf{u}) \ln(u_{11}^{-\theta_1} + u_{11}^{-\theta_1} - 1) + V(\boldsymbol{\theta}, \mathbf{u}) \ln(u_{21}^{-1}) \right\} \right\} \right| \\ &\quad \times \left[\left(\frac{\theta_1}{\theta_0} - 1 \right) + \frac{\left(u_{11}^{-\theta_1} + u_{12}^{-\theta_1} - 1 \right)^{\frac{\theta_0}{\theta_1}}}{\left\{ \left(u_{11}^{-\theta_1} + u_{12}^{-\theta_1} - 1 \right)^{\frac{\theta_0}{\theta_1}} + u_{21}^{-\theta_0} - 1 \right\}} \left(2 + \frac{1}{\theta_0} \right) \right]^{-1} \\ &\leq \left\{ \frac{1}{\theta_0^2} + \frac{2 + \theta_0^{-1}}{\theta_1} \ln(u_{11}^{-\theta_1} + u_{12}^{-\theta_1} - 1) + \left(2 + \frac{1}{\theta_0} \right) \left\{ \theta_1^{-1} \ln(u_{11}^{-\theta_1} + u_{12}^{-\theta_1} - 1) + \ln(u_{21}^{-1}) \right\} \right\}, \end{aligned}$$

and

$$\begin{aligned} \left| \frac{\partial}{\partial \theta_1} \ln(E(\boldsymbol{\theta}, \mathbf{u})) \right| &= \left| \frac{2\theta_0 + 1}{\theta_1 - \theta_0} W(\boldsymbol{\theta}, \mathbf{u}) \left\{ \frac{Z(\boldsymbol{\theta}, \mathbf{u}) - W(\boldsymbol{\theta}, \mathbf{u})Z(\boldsymbol{\theta}, \mathbf{u}) - 1}{1 + \frac{2\theta_0 + 1}{\theta_1 - \theta_0} W(\boldsymbol{\theta}, \mathbf{u})} \right\} \right| \\ &\leq 2 \frac{2\theta_0 + 1}{\theta_1 - \theta_0} |Z(\boldsymbol{\theta}, \mathbf{u})| \\ &\leq \frac{4\theta_0 + 2}{\theta_1 - \theta_0} \left\{ \ln(u_{11}^{-1}) + \ln(u_{12}^{-1}) + \theta_1^{-1} \ln(u_{12}^{-1} + u_{12}^{-1}) \right\}. \end{aligned}$$

Therefore taking $\epsilon < (\theta_1 - \theta_0)/2$ we get that the derivatives are bounded in a neighborhood of the true parameter, which we can use as the Lipszhit constant.

Integrability of the envelope function. It is sufficient to check that all of the following functions are integrable with respect to the true data generating density: $\ln(u_{11}^{-\theta_1} + u_{12}^{-\theta_1})^2$, $\ln(u_{11}^{-\theta_1} + u_{12}^{-\theta_1} + u_{21}^{-\theta_0})^2$, $\ln(u_{11})^2$, $\ln(u_{12})^2$, $\ln(u_{21})^2$ (as $E[\ln(u_{11})]^2 < E \ln(u_{11})^2$ by Jensen's inequality) under the null of $\theta_0 = \theta_1$. Note that the marginal distribution of each individual u_{11}, u_{12}, u_{21} are uniform $[0, 1]$. Therefore:

$$\int_0^1 \ln(u_{21})^2 du_{21} < \infty.$$

Since $\ln(u_{11}^{-\theta_1} + u_{12}^{-\theta_1}) \leq \ln(2u_{11}^{-\theta_1}) + \ln(2u_{12}^{-\theta_1})$ on the unit square, and the fact that $x^2 + y^2 > 2xy$ for real numbers x, y therefore:

$$\int_0^1 \int_0^1 \ln(u_{11}^{-\theta_1} + u_{12}^{-\theta_1})^2 dC_{\boldsymbol{\theta}} \leq 2 \int_0^1 \ln(2u_{11}^{-\theta_1})^2 du_{11} + 2 \int_0^1 \ln(2u_{12}^{-\theta_1})^2 du_{12} < \infty$$

for all $\theta_1 > 0$, and for $\theta_1 = \theta_0$. A similar result can be shown for the expectation of $\ln(u_{11}^{-\theta_1} + u_{12}^{-\theta_1} + u_{21}^{-\theta_0})^2$.

D Additional material for § 4

sigma-estimation

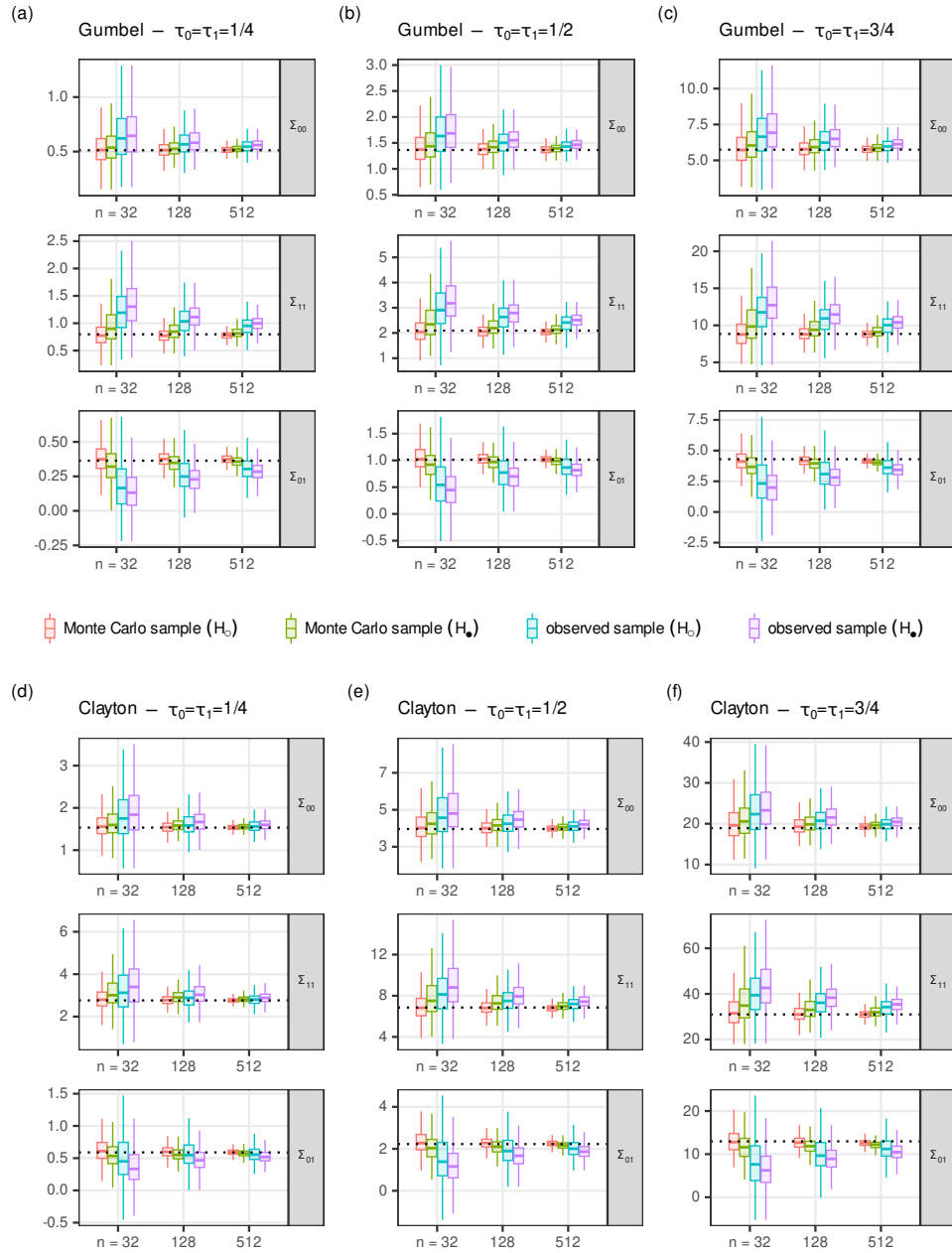


Figure D.1: Boxplots comparing four estimators of Σ_{00} based on the methodology of §4 for a Gumbel (a-c) and Clayton (d-f) HACs with structure $\{\{1, 2\}, 3\}$ and three pairs of identical parameters: $(\vartheta_0, \vartheta_1) = (\vartheta, \vartheta)$ with $\vartheta \in \{\theta : \tau_\psi(\theta) = 1/4, 1/2, 3/4\}$; the null hypothesis is $H_0 : \vartheta_0 = \vartheta_1$. The four estimators are obtained by considering either $\hat{\theta}_o$ (H_o) or $\hat{\theta}_\bullet$ (H_\bullet), and either the observed sample (of size n) or a Monte Carlo sample (of size $N = 10^5$) generated from $C_{\hat{\theta}}$. The dashed lines indicate the true value of Σ_{00} , approximated using Monte Carlo sampling and the explicit formulas given in Appendix B

sigma-full

E Results of the simulation study

op:sim-study

Simple hypothesis – likelihood ratio test

Model	Gumbel data			Clayton data			Frank data		
	n = 32	128	512	n = 32	128	512	n = 32	128	512
Gumbel	4	5	4	6	10	21	7	7	11
Clayton	6	5	7	4	5	6	6	7	8
Frank	6	5	6	8	10	13	6	4	5
Case a: $\tau_0 = \tau_1 = 1/4$									
Gumbel	5	5	5	11	16	37	8	9	15
Clayton	8	15	31	4	4	4	10	19	45
Frank	5	5	7	7	10	20	5	6	5
Case b: $\tau_0 = \tau_1 = 1/2$									
Gumbel	4	6	6	17	32	68	10	20	48
Clayton	16	32	70	5	4	6	24	54	94
Frank	6	8	13	10	16	32	4	4	4
Case c: $\tau_0 = \tau_1 = 3/4$									
Gumbel	27	73	99	23	50	94	23	51	96
Clayton	18	42	89	32	73	100	18	42	88
Frank	24	61	98	27	65	99	26	62	99
Case d: $\tau_0 = 1/4 < \tau_1 = 1/4 + 1/10$									
Gumbel	47	93	100	33	74	99	34	77	100
Clayton	36	72	99	53	95	100	33	71	99
Frank	41	89	100	43	91	100	44	89	100
Case e: $\tau_0 = 1/2 < \tau_1 = 1/2 + 1/10$									
Gumbel	93	100	100	72	100	100	78	100	100
Clayton	78	100	100	94	100	100	67	98	100
Frank	90	100	100	90	100	100	92	100	100
Case f: $\tau_0 = 3/4 < \tau_1 = 3/4 + 1/10$									

Table E.1: Size (a–c) and power (d–f) in finite samples of the (unconditional) test of $H_0 : \vartheta_0 = \vartheta_1$ based on Corollary 1. The tree structure is set to $\mathcal{G} = \{\{1, 2\}, 3\}$ (two parameters) and three generator families (Gumbel, Clayton and Frank) and various values of $\vartheta_0 = \tau_\psi^{-1}(\tau_0)$ and $\vartheta_1 = \tau_\psi^{-1}(\tau_1)$ (as described in Section 3.2) are considered. The same three generator families are considered for modeling the data. Rejection rates are reported in %.

imple-uncond

Simple hypothesis – conditional likelihood ratio test

Model	Gumbel data			Clayton data			Frank data		
	n = 32	128	512	n = 32	128	512	n = 32	128	512
Gumbel	2	3	2	4	6	14	3	4	6
Clayton	3	2	4	2	3	3	4	4	5
Frank	3	3	3	4	6	8	3	1	3
Case a: $\tau_0 = \tau_1 = 1/4$									
Gumbel	2	2	3	7	11	28	5	5	11
Clayton	4	9	23	2	2	2	6	13	35
Frank	3	3	4	4	6	13	3	2	3
Case b: $\tau_0 = \tau_1 = 1/2$									
Gumbel	2	2	3	11	26	60	7	15	40
Clayton	11	26	62	2	2	3	18	47	91
Frank	4	4	8	6	11	23	2	2	2
Case c: $\tau_0 = \tau_1 = 3/4$									
Gumbel	20	62	99	16	41	91	15	38	92
Clayton	12	32	81	21	62	99	12	33	82
Frank	16	50	97	18	53	99	18	49	97
Case d: $\tau_0 = 1/4 < \tau_1 = 1/4 + 1/10$									
Gumbel	38	89	100	26	66	98	25	70	99
Clayton	26	65	98	40	92	100	25	64	99
Frank	32	82	100	32	85	100	32	83	100
Case e: $\tau_0 = 1/2 < \tau_1 = 1/2 + 1/10$									
Gumbel	88	100	100	65	99	100	72	100	100
Clayton	70	99	100	90	100	100	60	97	100
Frank	85	100	100	85	100	100	86	100	100
Case f: $\tau_0 = 3/4 < \tau_1 = 3/4 + 1/10$									

Table E.2: Size (a–c) and power (d–f) in finite samples of the conditional test of $H_o : \vartheta_0 = \vartheta_1$ based on Remark 3. The tree structure is set to $\mathcal{G} = \{\{1, 2\}, 3\}$ (two parameters) and three generator families (Gumbel, Clayton and Frank) and various values of $\vartheta_0 = \tau_\psi^{-1}(\tau_0)$ and $\vartheta_1 = \tau_\psi^{-1}(\tau_1)$ (as described in Section 3.2) are considered. The same three generator families are considered for modeling the data. Rejection rates are reported in %.

simple-cond

Intersection hypothesis – likelihood ratio test
 $\hat{\Sigma}$ computed at $\hat{\theta}_o$ using Monte Carlo sampling (10^5 replicates)

Model	Gumbel data			Clayton data			Frank data		
	n = 32	128	512	n = 32	128	512	n = 32	128	512
Gumbel	6	5	4	9	13	26	5	6	10
Clayton	7	6	7	6	5	4	7	7	8
Frank	6	5	4	7	10	22	4	5	4
Case a: $\tau_0 = \tau_1 = \tau_2 = 1/4$									
Gumbel	5	4	5	13	22	52	8	10	22
Clayton	10	21	53	5	5	5	15	37	82
Frank	7	6	9	9	11	28	4	4	5
Case b: $\tau_0 = \tau_1 = \tau_2 = 1/2$									
Gumbel	4	5	4	27	55	95	16	36	76
Clayton	27	63	98	4	5	6	51	94	100
Frank	6	9	16	12	25	52	5	4	4
Case c: $\tau_0 = \tau_1 = \tau_2 = 3/4$									
Gumbel	28	68	99	22	47	93	19	48	95
Clayton	17	37	87	27	72	100	18	39	91
Frank	21	60	99	25	65	100	24	56	98
Case d: $\tau_0 = \tau_1 = 1/4 < \tau_2 = 1/4 + 1/10$									
Gumbel	40	90	100	33	77	100	32	75	100
Clayton	37	79	100	44	95	100	40	84	100
Frank	40	87	100	42	93	100	37	90	100
Case e: $\tau_0 = \tau_1 = 1/2 < \tau_2 = 1/2 + 1/10$									
Gumbel	94	100	100	75	100	100	79	100	100
Clayton	86	100	100	94	100	100	83	100	100
Frank	90	100	100	91	100	100	91	100	100
Case f: $\tau_0 = \tau_1 = 3/4 < \tau_2 = 3/4 + 1/10$									
Gumbel	45	91	100	29	70	99	32	73	100
Clayton	26	62	99	47	94	100	29	67	100
Frank	39	86	100	40	87	100	37	84	100
Case g: $\tau_0 = 1/4 < \tau_1 = \tau_2 = 1/4 + 1/10$									
Gumbel	71	100	100	52	93	100	55	95	100
Clayton	56	98	100	75	100	100	59	98	100
Frank	65	99	100	63	100	100	66	99	100
Case h: $\tau_0 = 1/2 < \tau_1 = \tau_2 = 1/2 + 1/10$									
Gumbel	100	100	100	94	100	100	94	100	100
Clayton	97	100	100	100	100	100	97	100	100
Frank	99	100	100	99	100	100	99	100	100
Case i: $\tau_0 = 3/4 < \tau_1 = \tau_2 = 3/4 + 1/10$									

Table E.3: Size (a–c) and power (d–i) in finite samples of the (unconditional) test of $H_o : \vartheta_0 = \vartheta_1 = \vartheta_2$ based on Corollary 2, using the estimator of Σ computed at the null parameter ($\hat{\theta}_o$) based on a Monte Carlo sample (10^5 replicates) from the null model. The tree structure is set to $\mathcal{G} = \{\{1, 2\}, \{3, 4\}\}$ (three parameters) and three generator families (Gumbel, Clayton and Frank) and various values of $\vartheta_i = \tau_\psi^{-1}(\tau_i)$ ($i = 0, 1, 2$; as described in Section 3.2) are considered. The same three generator families are considered for modeling the data. Rejection rates are reported in %.

Intersection hypothesis – likelihood ratio test
 $\hat{\Sigma}$ computed at $\hat{\theta}_\bullet$ using Monte Carlo sampling (10^5 replicates)

Model	Gumbel data			Clayton data			Frank data		
	n = 32	128	512	n = 32	128	512	n = 32	128	512
Gumbel	9	9	7	13	18	33	9	9	14
Clayton	10	11	11	9	7	8	11	10	12
Frank	9	9	8	11	16	31	7	8	8
Case a: $\tau_0 = \tau_1 = \tau_2 = 1/4$									
Gumbel	8	7	9	20	30	62	12	15	30
Clayton	16	31	63	7	8	9	20	46	88
Frank	10	10	13	13	19	38	8	7	9
Case b: $\tau_0 = \tau_1 = \tau_2 = 1/2$									
Gumbel	6	8	7	33	61	96	22	44	82
Clayton	35	70	99	8	8	8	57	96	100
Frank	11	15	24	19	33	63	8	7	6
Case c: $\tau_0 = \tau_1 = \tau_2 = 3/4$									
Gumbel	36	75	100	28	56	95	26	57	97
Clayton	24	47	92	34	80	100	24	49	95
Frank	26	68	100	33	74	100	30	66	99
Case d: $\tau_0 = \tau_1 = 1/4 < \tau_2 = 1/4 + 1/10$									
Gumbel	48	94	100	42	84	100	42	82	100
Clayton	44	85	100	52	97	100	48	90	100
Frank	50	92	100	50	95	100	46	93	100
Case e: $\tau_0 = \tau_1 = 1/2 < \tau_2 = 1/2 + 1/10$									
Gumbel	96	100	100	83	100	100	84	100	100
Clayton	88	100	100	97	100	100	88	100	100
Frank	93	100	100	94	100	100	94	100	100
Case f: $\tau_0 = \tau_1 = 3/4 < \tau_2 = 3/4 + 1/10$									
Gumbel	53	93	100	39	76	100	41	80	100
Clayton	35	72	100	56	96	100	36	75	100
Frank	48	91	100	50	91	100	46	90	100
Case g: $\tau_0 = 1/4 < \tau_1 = \tau_2 = 1/4 + 1/10$									
Gumbel	78	100	100	61	96	100	63	97	100
Clayton	64	98	100	80	100	100	68	99	100
Frank	72	99	100	72	100	100	74	100	100
Case h: $\tau_0 = 1/2 < \tau_1 = \tau_2 = 1/2 + 1/10$									
Gumbel	100	100	100	96	100	100	96	100	100
Clayton	98	100	100	100	100	100	98	100	100
Frank	99	100	100	99	100	100	99	100	100
Case i: $\tau_0 = 3/4 < \tau_1 = \tau_2 = 3/4 + 1/10$									

Table E.4: Size (a–c) and power (d–i) in finite samples of the (unconditional) test of $H_0 : \vartheta_0 = \vartheta_1 = \vartheta_2$ based on Corollary 2, using the estimator of Σ computed at the alternative parameter ($\hat{\theta}_\bullet$) based on a Monte Carlo sample (10^5 replicates) from the alternative model. The tree structure is set to $\mathcal{G} = \{\{1, 2\}, \{3, 4\}\}$ (three parameters) and three generator families (Gumbel, Clayton and Frank) and various values of $\vartheta_i = \tau_\psi^{-1}(\tau_i)$ ($i = 0, 1, 2$; as described in Section 3.2) are considered. The same three generator families are considered for modeling the data. Rejection rates are reported in %.

Intersection hypothesis – likelihood ratio test

$\hat{\Sigma}$ computed at $\hat{\theta}_o$ based on the observed data

Model	Gumbel data			Clayton data			Frank data		
	n = 32	128	512	n = 32	128	512	n = 32	128	512
Gumbel	6	5	4	9	13	26	5	6	10
Clayton	7	7	7	6	5	4	8	7	8
Frank	6	5	5	7	11	22	4	5	4
Case a: $\tau_0 = \tau_1 = \tau_2 = 1/4$									
Gumbel	5	4	5	13	23	52	8	10	22
Clayton	10	21	53	5	5	5	15	37	82
Frank	7	6	9	9	11	28	5	4	5
Case b: $\tau_0 = \tau_1 = \tau_2 = 1/2$									
Gumbel	4	5	4	27	55	95	16	36	76
Clayton	27	63	98	4	5	6	50	94	100
Frank	6	9	16	12	25	52	5	4	4
Case c: $\tau_0 = \tau_1 = \tau_2 = 3/4$									
Gumbel	28	68	99	22	48	93	19	48	95
Clayton	18	38	87	27	72	100	18	40	91
Frank	21	60	99	25	65	100	24	57	99
Case d: $\tau_0 = \tau_1 = 1/4 < \tau_2 = 1/4 + 1/10$									
Gumbel	41	90	100	33	77	100	32	75	100
Clayton	37	79	100	45	95	100	40	84	100
Frank	40	88	100	42	93	100	37	90	100
Case e: $\tau_0 = \tau_1 = 1/2 < \tau_2 = 1/2 + 1/10$									
Gumbel	94	100	100	75	100	100	79	100	100
Clayton	86	100	100	94	100	100	83	100	100
Frank	90	100	100	91	100	100	92	100	100
Case f: $\tau_0 = \tau_1 = 3/4 < \tau_2 = 3/4 + 1/10$									
Gumbel	45	91	100	29	70	99	32	74	100
Clayton	27	63	99	48	94	100	29	68	100
Frank	40	86	100	40	87	100	37	84	100
Case g: $\tau_0 = 1/4 < \tau_1 = \tau_2 = 1/4 + 1/10$									
Gumbel	72	100	100	52	93	100	56	95	100
Clayton	57	98	100	75	100	100	60	98	100
Frank	65	99	100	64	100	100	66	99	100
Case h: $\tau_0 = 1/2 < \tau_1 = \tau_2 = 1/2 + 1/10$									
Gumbel	100	100	100	94	100	100	94	100	100
Clayton	97	100	100	100	100	100	97	100	100
Frank	99	100	100	99	100	100	99	100	100
Case i: $\tau_0 = 3/4 < \tau_1 = \tau_2 = 3/4 + 1/10$									

Table E.5: Size (a–c) and power (d–i) in finite samples of the (unconditional) test of $H_o : \vartheta_0 = \vartheta_1 = \vartheta_2$ based on Corollary 2, using the estimator of Σ computed at the null parameter ($\hat{\theta}_o$) based on the observed sample. The tree structure is set to $\mathcal{G} = \{\{1, 2\}, \{3, 4\}\}$ (three parameters) and three generator families (Gumbel, Clayton and Frank) and various values of $\vartheta_i = \tau_{\psi}^{-1}(\tau_i)$ ($i = 0, 1, 2$; as described in Section 3.2) are considered. The same three generator families are considered for modeling the data. Rejection rates are reported in %.

b:int-0-obs

Intersection hypothesis – likelihood ratio test

$\hat{\Sigma}$ computed at $\hat{\theta}_\bullet$ based on the observed data

Model	Gumbel data			Clayton data			Frank data		
	n = 32	128	512	n = 32	128	512	n = 32	128	512
Gumbel	9	9	7	12	19	34	8	9	14
Clayton	10	11	11	10	7	8	11	10	12
Frank	9	9	8	10	16	30	7	8	8
Case a: $\tau_0 = \tau_1 = \tau_2 = 1/4$									
Gumbel	8	7	8	20	29	62	12	15	29
Clayton	16	31	64	7	8	9	21	46	88
Frank	10	10	13	12	18	38	8	7	8
Case b: $\tau_0 = \tau_1 = \tau_2 = 1/2$									
Gumbel	6	9	7	33	61	96	22	43	82
Clayton	35	70	99	7	8	8	58	96	100
Frank	11	15	24	18	33	63	9	7	6
Case c: $\tau_0 = \tau_1 = \tau_2 = 3/4$									
Gumbel	36	74	100	28	56	95	25	56	97
Clayton	24	47	92	34	79	100	23	50	95
Frank	26	68	100	33	74	100	30	66	99
Case d: $\tau_0 = \tau_1 = 1/4 < \tau_2 = 1/4 + 1/10$									
Gumbel	48	94	100	41	83	100	41	82	100
Clayton	44	85	100	52	97	100	49	90	100
Frank	49	92	100	50	95	100	46	94	100
Case e: $\tau_0 = \tau_1 = 1/2 < \tau_2 = 1/2 + 1/10$									
Gumbel	96	100	100	82	100	100	83	100	100
Clayton	88	100	100	97	100	100	88	100	100
Frank	93	100	100	94	100	100	94	100	100
Case f: $\tau_0 = \tau_1 = 3/4 < \tau_2 = 3/4 + 1/10$									
Gumbel	53	93	100	38	76	100	40	80	100
Clayton	36	72	100	56	96	100	37	75	100
Frank	48	91	100	49	91	100	47	90	100
Case g: $\tau_0 = 1/4 < \tau_1 = \tau_2 = 1/4 + 1/10$									
Gumbel	78	100	100	60	96	100	62	97	100
Clayton	64	98	100	81	100	100	68	99	100
Frank	73	99	100	71	100	100	74	100	100
Case h: $\tau_0 = 1/2 < \tau_1 = \tau_2 = 1/2 + 1/10$									
Gumbel	100	100	100	96	100	100	96	100	100
Clayton	98	100	100	100	100	100	98	100	100
Frank	99	100	100	99	100	100	99	100	100
Case i: $\tau_0 = 3/4 < \tau_1 = \tau_2 = 3/4 + 1/10$									

Table E.6: Size (a–c) and power (d–i) in finite samples of the (unconditional) test of $H_o : \vartheta_0 = \vartheta_1 = \vartheta_2$ based on Corollary 2, using the estimator of Σ computed at the alternative parameter ($\hat{\theta}_\bullet$) based on the observed sample. The tree structure is set to $\mathcal{G} = \{\{1, 2\}, \{3, 4\}\}$ (three parameters) and three generator families (Gumbel, Clayton and Frank) and various values of $\vartheta_i = \tau_\psi^{-1}(\tau_i)$ ($i = 0, 1, 2$; as described in Section 3.2) are considered. The same three generator families are considered for modeling the data. Rejection rates are reported in %.

b:int-1-obs

Union hypothesis – likelihood ratio test

Model	Gumbel data			Clayton data			Frank data		
	n = 32	128	512	n = 32	128	512	n = 32	128	512
Gumbel	1	0	0	0	1	3	0	0	0
Clayton	0	0	0	0	0	0	0	0	1
Frank	0	0	0	1	1	4	0	0	0
Case a: $\tau_0 = \tau_1 = \tau_2 = 1/4$									
Gumbel	0	0	0	1	3	14	0	1	3
Clayton	0	0	8	0	0	0	1	2	24
Frank	0	0	1	0	1	3	0	0	1
Case b: $\tau_0 = \tau_1 = \tau_2 = 1/2$									
Gumbel	0	0	0	2	15	63	1	6	33
Clayton	2	12	70	0	0	0	3	45	99
Frank	0	0	2	1	3	14	0	0	0
Case c: $\tau_0 = \tau_1 = \tau_2 = 3/4$									
Gumbel	1	4	5	2	5	17	1	3	8
Clayton	1	3	6	2	6	4	1	4	6
Frank	1	4	6	2	8	14	2	4	6
Case d: $\tau_0 = \tau_1 = 1/4 < \tau_2 = 1/4 + 1/10$									
Gumbel	2	3	6	4	14	36	2	7	18
Clayton	3	11	36	3	4	5	3	15	59
Frank	2	6	6	4	13	20	3	4	4
Case e: $\tau_0 = \tau_1 = 1/2 < \tau_2 = 1/2 + 1/10$									
Gumbel	5	4	5	13	38	80	9	25	59
Clayton	14	40	82	4	4	4	17	68	98
Frank	6	9	13	10	18	37	4	4	5
Case f: $\tau_0 = \tau_1 = 3/4 < \tau_2 = 3/4 + 1/10$									
Gumbel	13	56	100	5	26	90	6	30	93
Clayton	4	19	83	14	61	100	4	20	88
Frank	8	45	99	10	49	100	8	45	99
Case g: $\tau_0 = 1/4 < \tau_1 = \tau_2 = 1/4 + 1/10$									
Gumbel	28	90	100	16	61	100	15	68	100
Clayton	13	61	100	32	94	100	10	55	100
Frank	22	87	100	22	87	100	25	88	100
Case h: $\tau_0 = 1/2 < \tau_1 = \tau_2 = 1/2 + 1/10$									
Gumbel	89	100	100	58	98	100	69	99	100
Clayton	65	100	100	92	100	100	48	97	100
Frank	84	100	100	84	100	100	89	100	100
Case i: $\tau_0 = 3/4 < \tau_1 = \tau_2 = 3/4 + 1/10$									

Table E.7: Size (a–e) and power (f–i) in finite samples of the (unconditional) test of $H_0 : \vartheta_0 \in \{\vartheta_1, \vartheta_2\}$ based on Corollary 3 (reference distribution: $W_1\chi_1^2$ with $W_1 \sim \mathcal{B}(1/2)$). The tree structure is set to $\mathcal{G} = \{\{1, 2\}, \{3, 4\}\}$ (three parameters) and three generator families (Gumbel, Clayton and Frank) and various values of $\vartheta_i = \tau_\psi^{-1}(\tau_i)$ ($i = 0, 1, 2$; as described in Section 3.2) are considered. The same three generator families are considered for modeling the data. Rejection rates are reported in %.

tab:union

Simple hypothesis w/ nuisance – likelihood ratio test (assuming $\vartheta_0 = \vartheta_2$)
Cases a–f

Model	Gumbel data			Clayton data			Frank data		
	n = 32	128	512	n = 32	128	512	n = 32	128	512
Gumbel	6	5	3	8	10	22	7	7	10
Clayton	6	6	7	5	6	6	6	8	10
Frank	4	6	5	6	10	14	4	5	5
Case a: $\tau_0 = \tau_1 = \tau_2 = 1/4$									
Gumbel	5	4	6	10	18	38	6	9	16
Clayton	10	16	38	6	5	5	13	26	56
Frank	5	6	9	8	11	20	5	5	5
Case b: $\tau_0 = \tau_1 = \tau_2 = 1/2$									
Gumbel	4	4	4	19	38	77	13	25	59
Clayton	22	44	83	6	4	6	33	70	99
Frank	7	6	16	13	18	39	5	5	6
Case c: $\tau_0 = \tau_1 = \tau_2 = 3/4$									
Gumbel	6	5	4	8	10	18	5	7	7
Clayton	6	5	9	5	6	6	6	7	10
Frank	5	4	6	6	8	14	6	6	5
Case d: $\tau_0 = \tau_1 = 1/4 < \tau_2 = 1/4 + 1/10$									
Gumbel	5	6	6	12	17	40	9	11	17
Clayton	10	20	43	6	7	10	12	29	65
Frank	5	6	10	8	12	22	5	6	6
Case e: $\tau_0 = \tau_1 = 1/2 < \tau_2 = 1/2 + 1/10$									
Gumbel	6	8	8	19	41	80	17	26	61
Clayton	20	46	86	6	7	10	34	71	99
Frank	7	12	20	13	19	46	5	6	10
Case f: $\tau_0 = \tau_1 = 3/4 < \tau_2 = 3/4 + 1/10$									

Table E.8: Size (power in Figure E.9) in finite samples of the (unconditional) test of $H_0 : \vartheta_0 = \vartheta_1$ based on Corollary 1. The tree structure is set to $\mathcal{G} = \{\{1, 2\}, \{3, 4\}\}$ (three parameters, ϑ_2 is nuisance) and three generator families (Gumbel, Clayton and Frank) and various values of $\vartheta_i = \tau_\psi^{-1}(\tau_i)$ ($i = 0, 1, 2$; as described in Section 3.2) are considered. During the testing procedure, it is assumed that $\vartheta_2 = \vartheta_0$. The same three generator families are considered for modeling the data. Rejection rates are reported in %.

simplified-1

Simple hypothesis w/ nuisance – likelihood ratio test (assuming $\vartheta_0 = \vartheta_2$)
Cases k–l

Model	Gumbel data			Clayton data			Frank data		
	n = 32	128	512	n = 32	128	512	n = 32	128	512
Gumbel	33	74	100	26	55	96	23	57	96
Clayton	21	45	92	36	80	100	20	51	94
Frank	28	67	100	30	72	100	26	69	100
Case g: $\tau_0 = \tau_2 = 1/4 < \tau_1 = 1/4 + 1/10$									
Gumbel	55	95	100	39	78	100	39	83	100
Clayton	43	82	100	59	98	100	40	80	100
Frank	48	94	100	51	96	100	51	94	100
Case h: $\tau_0 = \tau_2 = 1/2 < \tau_1 = 1/2 + 1/10$									
Gumbel	95	100	100	80	100	100	82	100	100
Clayton	86	100	100	98	100	100	75	99	100
Frank	94	100	100	94	100	100	96	100	100
Case i: $\tau_0 = \tau_2 = 3/4 < \tau_1 = 3/4 + 1/10$									
Gumbel	33	75	100	22	51	94	22	53	96
Clayton	21	44	92	34	78	100	20	48	94
Frank	28	66	99	31	70	100	25	68	99
Case j: $\tau_0 = 1/4 < \tau_1 = \tau_2 = 1/4 + 1/10$									
Gumbel	56	94	100	38	78	100	41	81	100
Clayton	39	82	100	59	97	100	39	80	100
Frank	48	94	100	51	94	100	50	94	100
Case k: $\tau_0 = 1/2 < \tau_1 = \tau_2 = 1/2 + 1/10$									
Gumbel	96	100	100	74	100	100	82	100	100
Clayton	87	100	100	97	100	100	72	99	100
Frank	93	100	100	94	100	100	94	100	100
Case l: $\tau_0 = 3/4 < \tau_1 = \tau_2 = 3/4 + 1/10$									

Table E.9: Power (size in Figure E.8) in finite samples of the (unconditional) test of $H_0 : \vartheta_0 = \vartheta_1$ based on Corollary 1. The tree structure is set to $\mathcal{G} = \{\{1, 2\}, \{3, 4\}\}$ (three parameters, ϑ_2 is nuisance) and three generator families (Gumbel, Clayton and Frank) and various values of $\vartheta_i = \tau_\psi^{-1}(\tau_i)$ ($i = 0, 1, 2$; as described in Section 3.2) are considered. During the testing procedure, it is assumed that the $\vartheta_2 = \vartheta_0$. The same three generator families are considered for modeling the data.

simplified-2

**Simple hypothesis w/ nuisance – likelihood ratio test (hybrid)
Cases a–f**

Model	Gumbel data			Clayton data			Frank data		
	n = 32	128	512	n = 32	128	512	n = 32	128	512
Gumbel	5	5	3	8	10	22	7	7	10
Clayton	6	6	6	5	5	6	6	7	10
Frank	4	6	5	6	10	14	4	5	5
Case a: $\tau_0 = \tau_1 = \tau_2 = 1/4$									
Gumbel	5	3	5	10	18	38	6	9	16
Clayton	10	16	36	5	5	5	13	26	54
Frank	5	6	8	8	11	20	5	5	5
Case b: $\tau_0 = \tau_1 = \tau_2 = 1/2$									
Gumbel	4	4	4	19	38	77	13	25	59
Clayton	23	43	83	6	4	6	33	70	99
Frank	7	6	15	13	18	38	5	5	6
Case c: $\tau_0 = \tau_1 = \tau_2 = 3/4$									
Gumbel	6	5	4	8	10	19	6	7	8
Clayton	6	5	8	5	6	6	6	6	9
Frank	5	4	6	6	8	16	6	6	5
Case d: $\tau_0 = \tau_1 = 1/4 < \tau_2 = 1/4 + 1/10$									
Gumbel	4	5	4	11	17	38	8	10	16
Clayton	9	18	37	5	6	6	12	27	61
Frank	5	4	7	7	11	18	5	5	5
Case e: $\tau_0 = \tau_1 = 1/2 < \tau_2 = 1/2 + 1/10$									
Gumbel	5	5	4	18	39	78	15	24	57
Clayton	18	42	82	4	4	5	33	71	99
Frank	6	9	12	11	15	38	4	5	6
Case f: $\tau_0 = \tau_1 = 3/4 < \tau_2 = 3/4 + 1/10$									

Table E.10: Size (power in Figure E.11) in finite samples of the (unconditional) test of $H_0 : \vartheta_0 = \vartheta_1$ based on Remark 2. The tree structure is set to $\mathcal{G} = \{\{1, 2\}, \{3, 4\}\}$ (three parameters, ϑ_2 is nuisance) and three generator families (Gumbel, Clayton and Frank) and various values of $\vartheta_i = \tau_\psi^{-1}(\tau_i)$ ($i = 0, 1, 2$; as described in Section 3.2) are considered. The same three generator families are considered for modeling the data. Rejection rates are reported in %.

nce-hybrid-1

Simple hypothesis w/ nuisance – likelihood ratio test (hybrid)

Cases g–l

Model	Gumbel data			Clayton data			Frank data		
	n = 32	128	512	n = 32	128	512	n = 32	128	512
Gumbel	33	74	100	26	56	96	23	57	96
Clayton	21	45	92	36	80	100	20	50	94
Frank	28	67	100	30	72	100	26	69	100
Case g: $\tau_0 = \tau_2 = 1/4 < \tau_1 = 1/4 + 1/10$									
Gumbel	54	95	100	39	77	100	38	83	100
Clayton	42	81	100	58	98	100	40	78	99
Frank	48	93	100	51	96	100	50	94	100
Case h: $\tau_0 = \tau_2 = 1/2 < \tau_1 = 1/2 + 1/10$									
Gumbel	95	100	100	80	100	100	82	100	100
Clayton	85	100	100	98	100	100	74	99	100
Frank	93	100	100	93	100	100	96	100	100
Case i: $\tau_0 = \tau_2 = 3/4 < \tau_1 = 3/4 + 1/10$									
Gumbel	33	75	100	22	52	95	23	54	96
Clayton	21	44	92	34	78	100	20	48	94
Frank	28	65	99	31	70	100	25	68	99
Case j: $\tau_0 = 1/4 < \tau_1 = \tau_2 = 1/4 + 1/10$									
Gumbel	55	93	100	37	77	100	40	81	100
Clayton	38	80	100	57	97	100	38	79	100
Frank	47	92	100	50	93	100	49	93	100
Case k: $\tau_0 = 1/2 < \tau_1 = \tau_2 = 1/2 + 1/10$									
Gumbel	95	100	100	73	99	100	80	100	100
Clayton	85	100	100	96	100	100	72	99	100
Frank	92	100	100	93	100	100	93	100	100
Case l: $\tau_0 = 3/4 < \tau_1 = \tau_2 = 3/4 + 1/10$									

Table E.11: Power (size in Figure E.10) in finite samples of the (unconditional) test of $H_0 : \vartheta_0 = \vartheta_1$ based on Remark 2. The tree structure is set to $\mathcal{G} = \{\{1, 2\}, \{3, 4\}\}$ (three parameters, ϑ_2 is nuisance) and three generator families (Gumbel, Clayton and Frank) and various values of $\vartheta_i = \tau_\psi^{-1}(\tau_i)$ ($i = 0, 1, 2$; as described in Section 3.2) are considered. The same three generator families are considered for modeling the data. Rejection rates are reported in %.

ce-hybrid-2